COO-912-5

THE UNIVERSITY OF MICHIGAN
COLLEGE OF LITERATURE, SCIENCE, AND THE ARTS
Department of Chemistry
and
Michigan Memorial—Phoenix Project

Progress Report

ENERGETIC RECOIL ATOM REACTION MECHANISMS

Adon A. Gordus

ORA Project 03710

under contract with:

U. S. ATOMIC ENERGY COMMISSION
CONTRACT NO. AT(11-1)-912
ARGONNE, ILLINOIS

administered through:

OFFICE OF RESEARCH ADMINISTRATION ANN ARBOR

February 1965

I. SUMMARY OF RESEARCH PROGRAM

The research performed during the preceding year has been directed toward the understanding of high-energy atom and ion chemical reaction mechanisms. The major portion of the program was supported by the Atomic Energy Commission (Division of Research) funds. Substantial assistance was also received from The University of Michigan Department of Chemistry and the Michigan Memorial-Phoenix Project.

1. Undergraduate Assistants

Undergraduate Honors students continued to represent a major portion of the personnel. These students have, in general been assigned graduate-level research projects since they are capable of working at this level. However, the research performed by these students, because of their heavy course loads, must, of necessity, be at a slower pace. As a result, it may be two or three years before a significant and publishable amount of research is done by a student. In a few cases a student may graduate just at the time when only a few months more research would be needed to complete a project. Since University of Michigan Chemistry undergraduates have been encouraged to attend other graduate schools, these students and their many acquired research skills are "lost" to this program - but in the balance represent a very large net gain to the nation's science effort. In many cases these students do graduate research in areas supported by the Atomic Energy Commission.

Recently, the principal investigator was appointed Associate Director of The University of Michigan Honors program. As a result, he has an additional opportunity to identify, as incoming freshmen, those undergraduates who appear to be the most promising as research assistants. This year five freshmen were hired. They rank among the top 10-20 entering science students in a total freshman class of about 4,000. They are already started on (graduate level) research programs.

Attempts have always been made not to restrict an undergraduate's research activity to a narrow problem. Frequently a student would assist with a number of research projects before being assigned a project of his own. Recently, for example, all the students have been involved in the complete redesigning of much of the present experimental equipment, as well as in the decisions about the types of new equipment to be bought. Properly functioning equipment is, of course, a necessity in any research program, but when Honors undergraduates, with their limited time, are doing research it is even more imperative that the equipment function properly. In our research program, each experimental apparatus involves some type of major modification or design; a "black box" piece of equipment is never used except for spectrophotometric studies. Consequently, the students learn early the problems and frustrations associated with original research.

2. The Research Program

About a third of the research effort is devoted to high-energy chemical studies activated by nuclear reactions. Similar studies using photochemical activation currently comprise about

one-sixth of the total effort. The remaining effort is devoted to auxiliary problems. These include gas chromatographic separation of isotopically labeled compounds, determinations of the continuous ultraviolet absorption spectra of isotopically labeled gaseous molecules, and theoretical studies using digital and analog compouter techniques.

Results of one study enhance or are needed for the understanding of another study. For example, the gas chromatographic separations, while interesting and potentially significant as a separate study, are needed as an analytical detection method in the hot-atom studies. Similarly the UV spectral determinations, while of potential significance for future theoretical studies, are needed in order to design proper photochemical hot-atom studies

3. Facilities

Currently the research group has the use of three small (160 ft.^{2} each) labs and one medium-sized (558 ft.^{2}) lab in the Chemistry building and three labs (total area 554 ft.^{2}) in the Phoenix Memorial Laboratory which is connected to the reactor.

II. EXPERIMENTAL EQUIPMENT AND TECHNIQUES

As noted earlier, considerable effort has been and continues to be expended in the design and constructiom of experimental equipment. Such custom design is particularly necessary in the gas chromatography units since our research requirements are such that no commercial unit has the proper capabilities.

1. Isotope Separation Gas Chromatography

For these studies we frequently require column temperatures which may be as low as -196°C. For studies involving ^{12}CO - ^{13}CO separation we require a CO_2-to-CO converter. Figure 1 is a block diagram of a unit designed for a study of this latter separation. The columns are usually made of 50 foot lengths of 1/4" copper refrigeration tubing and we have constructed over 50 such columns with a variety of stationary phases or mixtures of stationary phases. A "Gow-Mac" thermal conductivity detector is used with this apparatus.

(W. Litzenberg)

2. Strong Beta-Radio Gas Chromatograph

A number of the experimental studies require analysis of strong beta-emitting hot-atom products. Since many of the products are high boiling a beta-detector capable of operating at temperatures of 200-300°C was needed. In some of these studies it is desirable to trap individually the radioactive gases separated by the gas chromatography column.

Figure 2 is a block diagram and Fig. 3 a photograph of a radio gas chromatograph designed according to the above requirements. Actually, this unit is not limited to strong-beta detection. As shown in Fig. 4, the heated radioactivity detector portion has been designed so that it can be easily replaced by a gamma-detecting unit. A photograph of this detecting portion of the unit is seen in Fig. 5

(B.G. Gibbard and M. Tsoukatos)

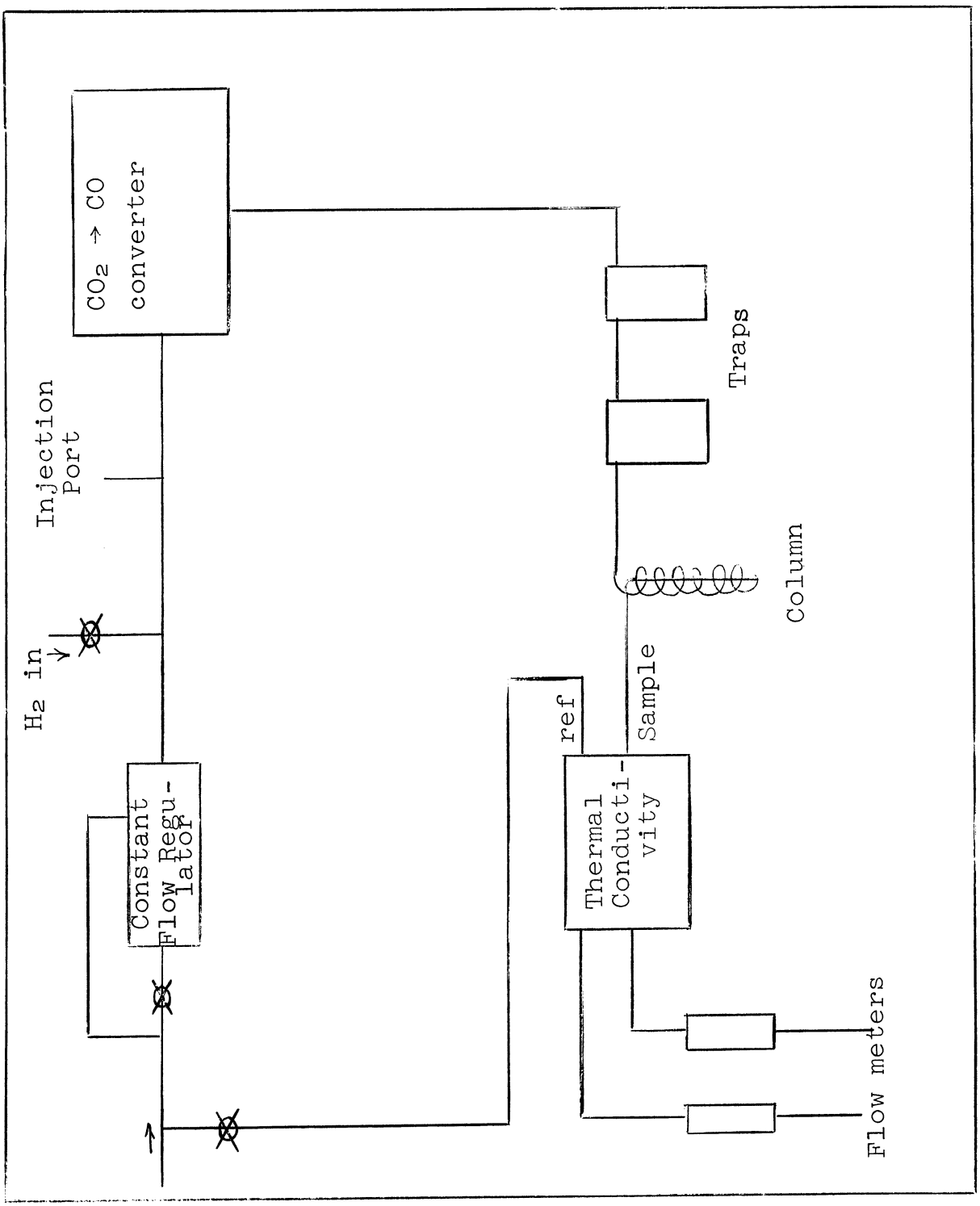

Figure 1. Block diagram of isotope-separation gas-chromatograph

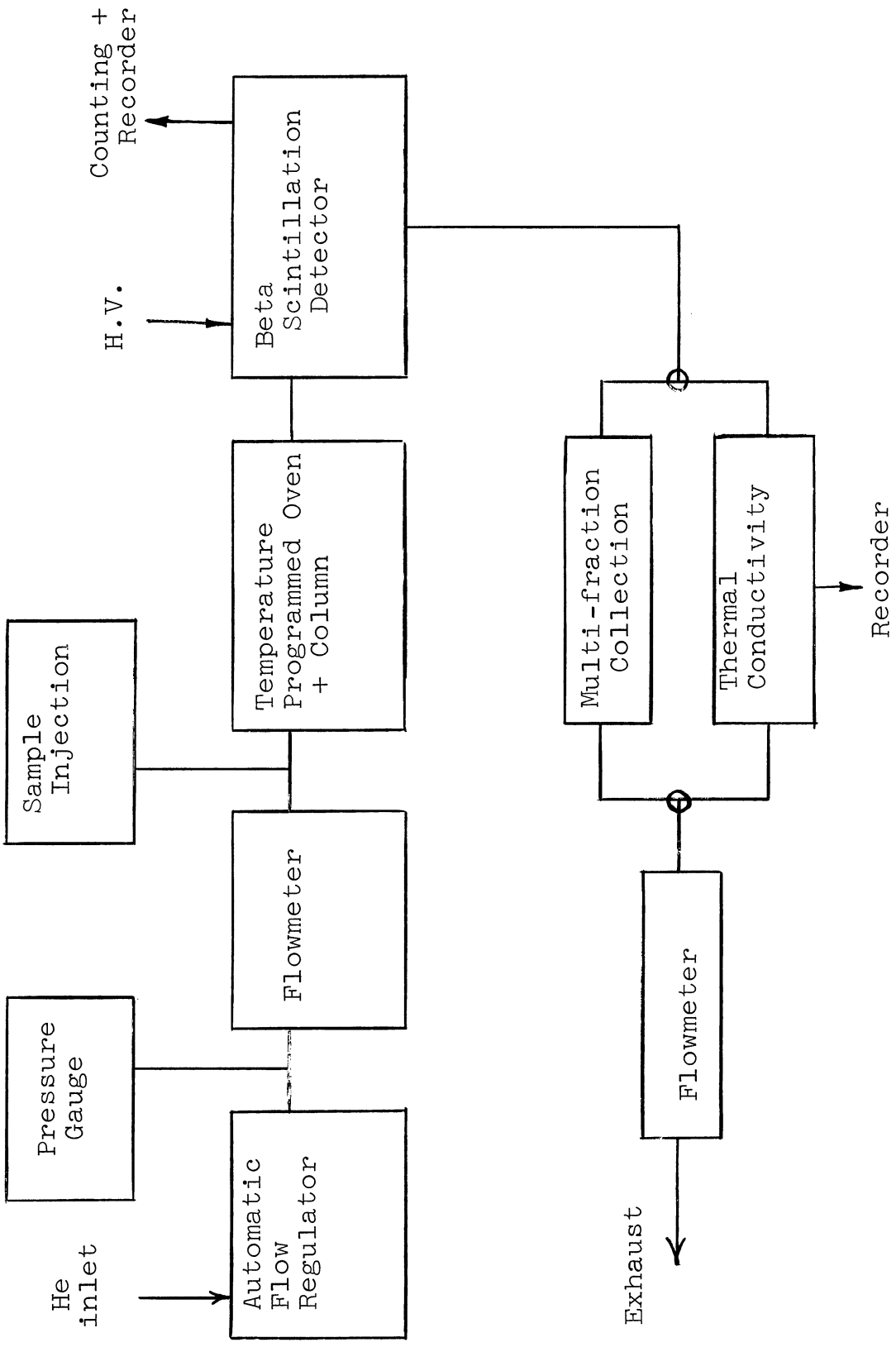

Figure 2. Block Diagram of strong beta-detecting radio gas chromatograph

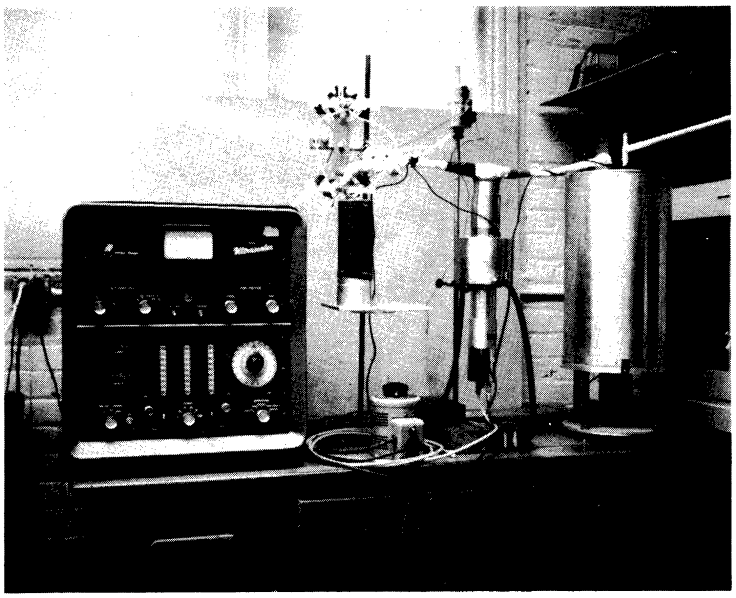

Figure 3. Radio-gas chromatograph diagrammed in Fig 2. (Thermal conductivity portion not shown.)

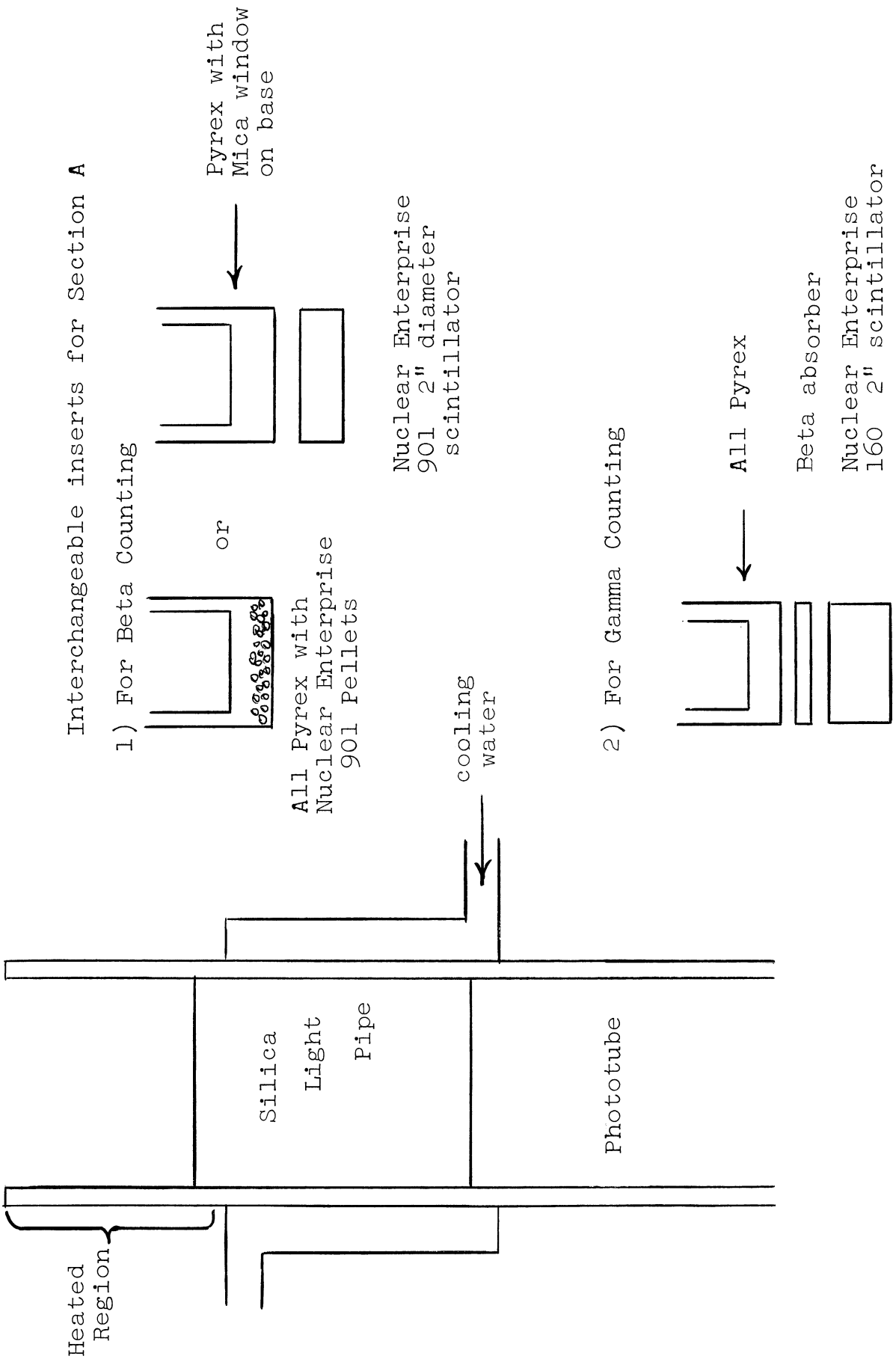

Figure 4. Schematic of high-temperature beta-detecting portion of Fig. 2.

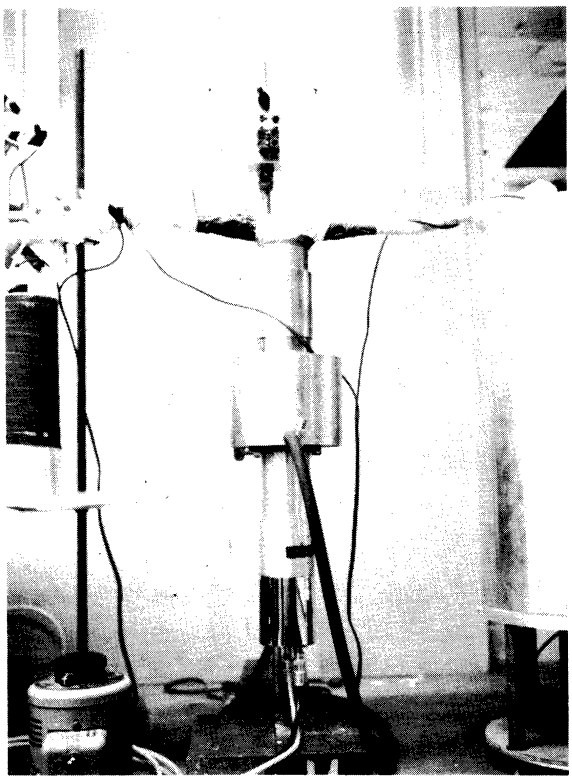

Figure 5. High-temperature beta-detecting portion of Fig. 2 with lead shielding and support removed.

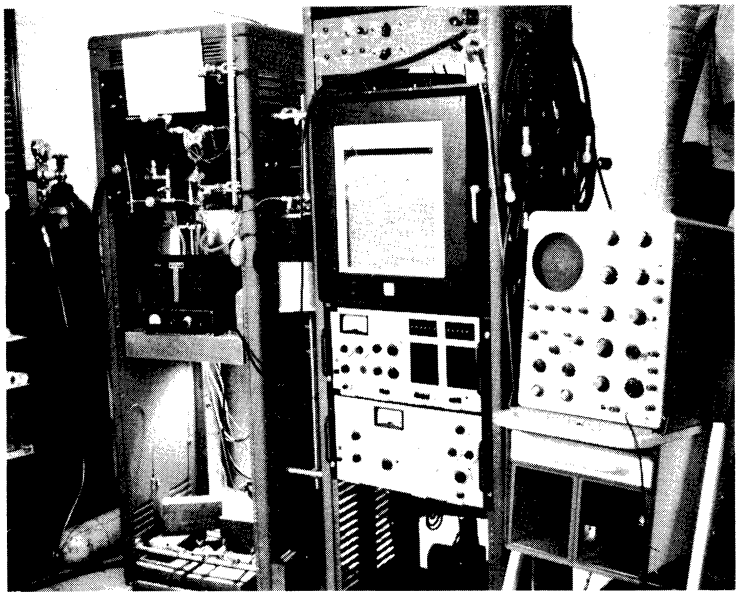

Figure 6. Tritium proportional-counting gas-chromatograph.

3. Tritium Proportional Counting Gas Chromatograph

A gas chromatograph with tritium detecting capabilities is needed in the isotope separation experiments, the $^3He(n,p)^3T$ hot-atom experiments, and in some of the photochemical hot-atom experiments.

The first flow proportional counting gas chromatograph developed was the (albeit crude) unit constructed by the principal investigator in 1956 while he was a graduate student at the University of Wisconsin. Since that time others, principally R. Wolfgang and F. S. Rowland, have developed tritium gas chromatography units of various degrees of sophistication. Recently a few nuclear equipment companies have marketed tritium detecting gas chromatographs. We have designed what, for our purposes, is a most accurate, rugged, and easily used tritium gas chromatograph. It is pictured in Fig. 6. The gas flow system is diagrammed in Fig. 7 and shown in Fig. 8.

Figure 9 is a photograph of a sample tube, the construction of which was based on the article by M. E. Bednas and D. S. Russell, [Can. J. Chem., 42, 1249 (1964).] This design permits the introduction of a sample without interrupting the gas flow or introducing air into the system.

The electronics used in conjunction with the gas chromatograph consist of a thermal conductivity cell and related circuitry, a flow proportional counting tube with power supply, amplifiers, scaling circuits, and a two pen recorder with an event marking pen. The counting circuit is diagrammed in Fig. 10 and the solid-state circuit portion shown in Fig. 11.

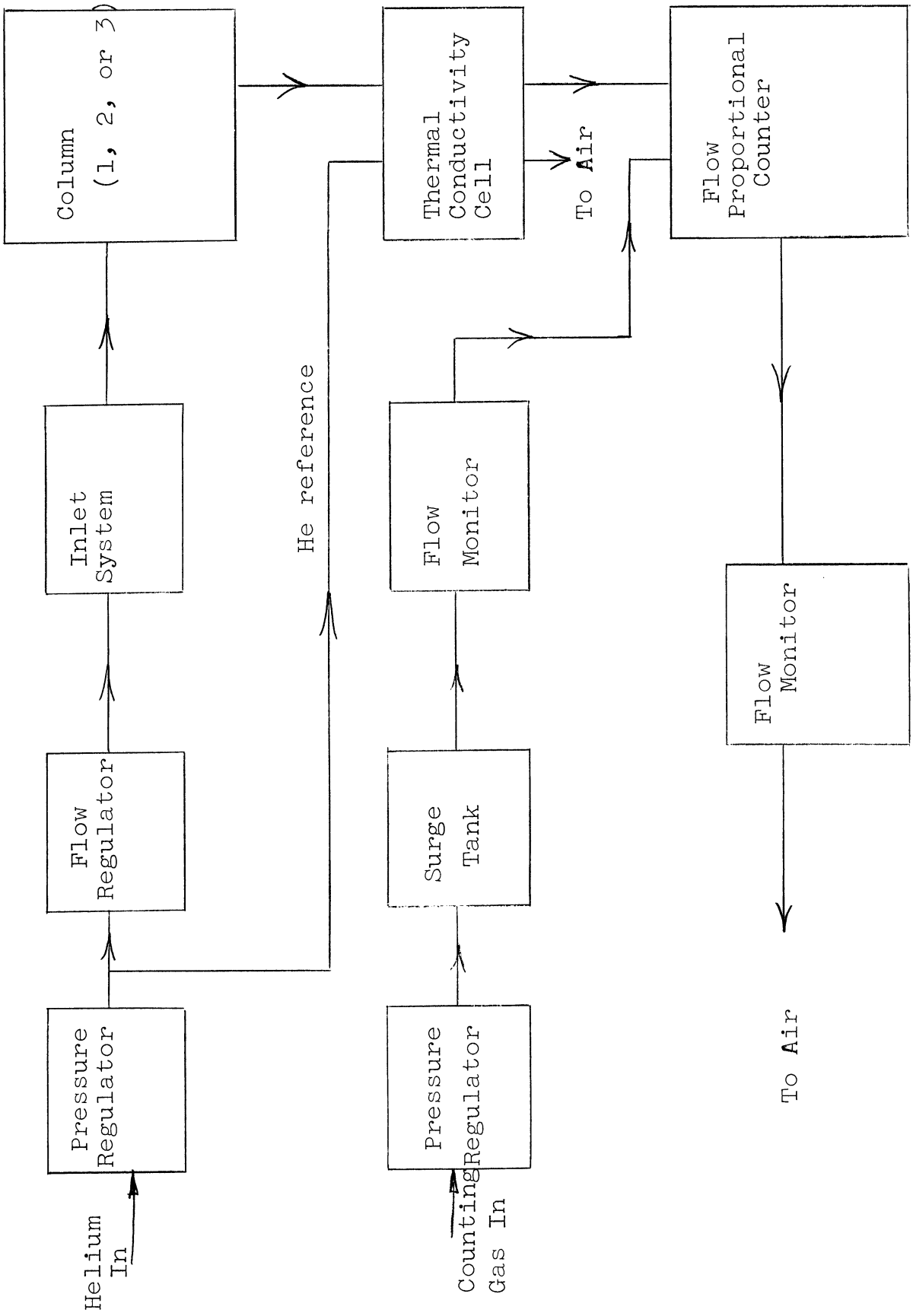

Figure 7. Block diagram of gas flow in tritium gas chromatograph

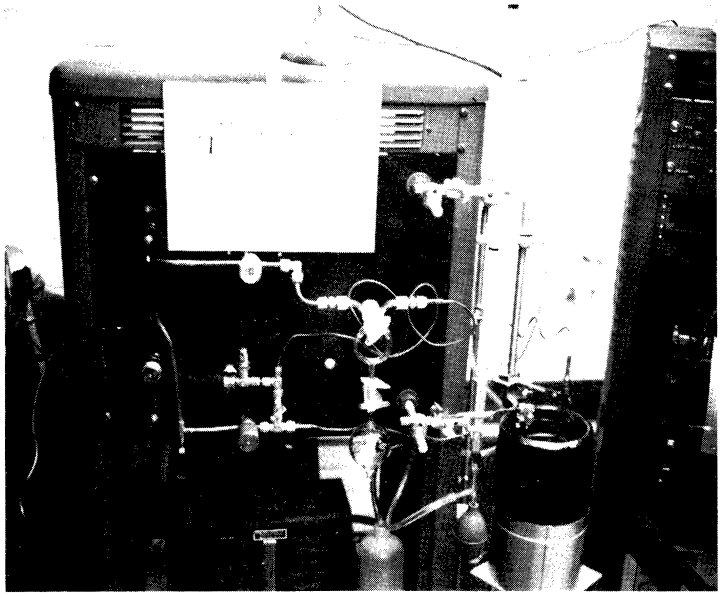

Figure 8. Gas flow section of tritium gas-chromatograph.

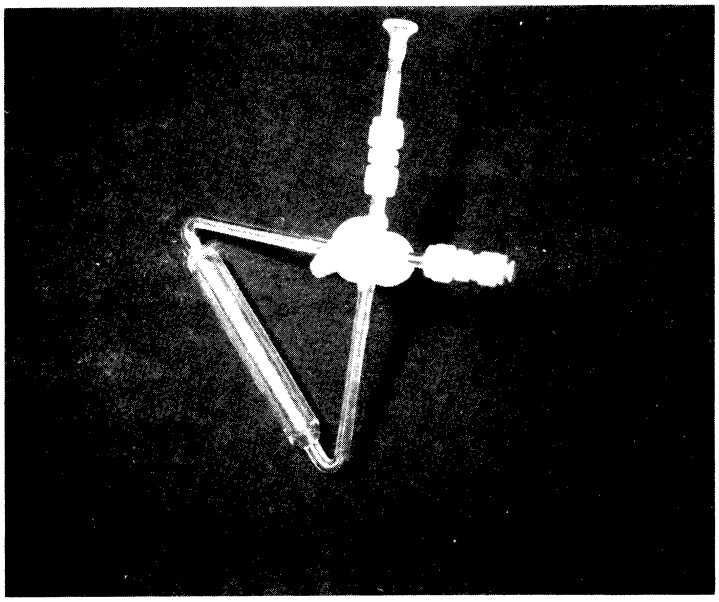

Figure 9. Sample tube for tritium gas-chromatography.

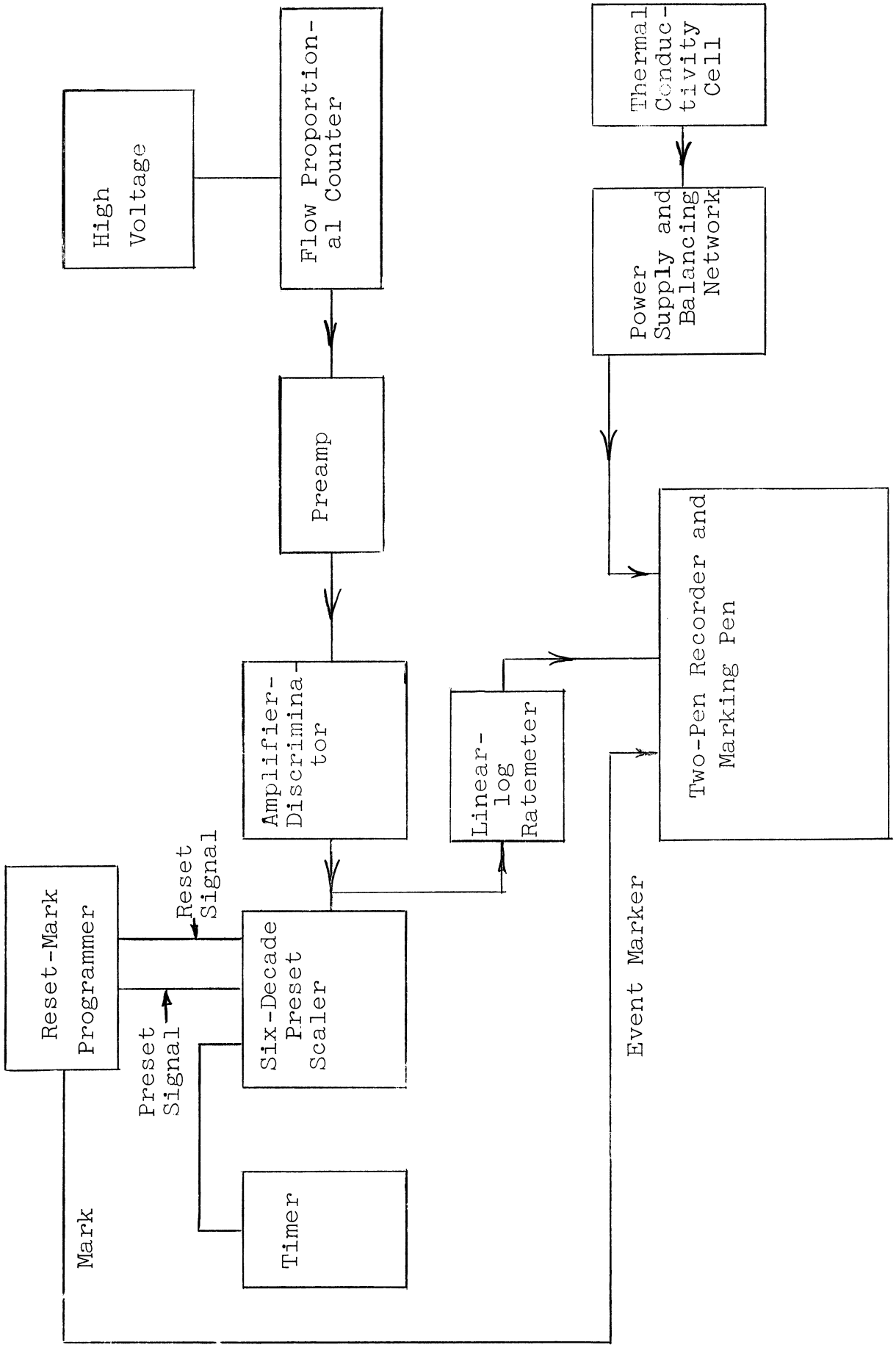

Figure 10. Block diagram of counting circuits for tritium gas chromatograph

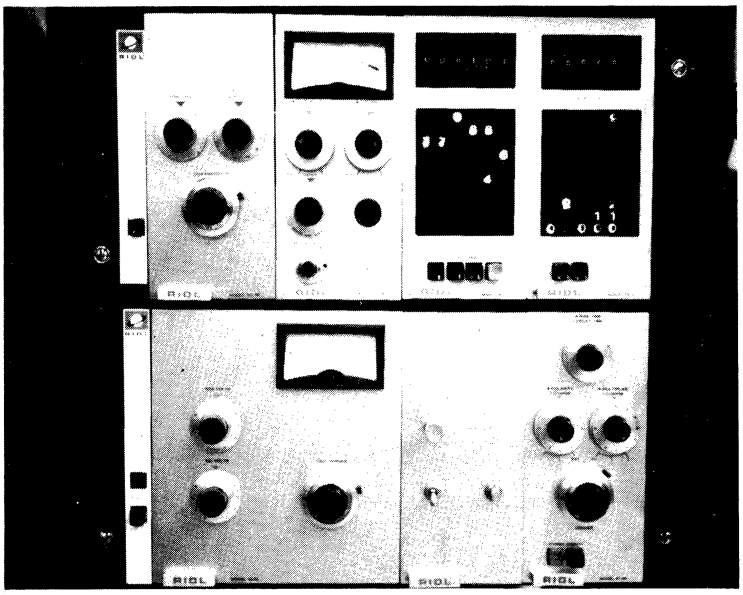

Figure 11. Solid-state circuit portion of tritium gas-chromatograph.

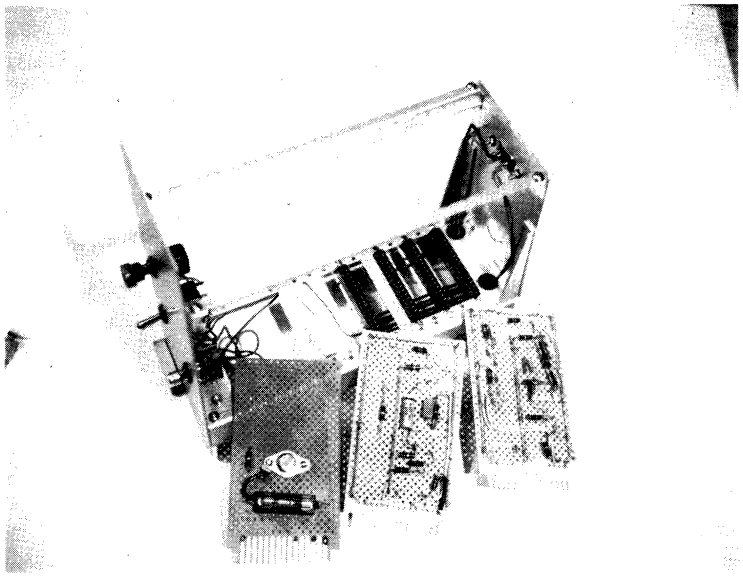

Figure 12. Home-built solid-state reset, event-marking programmer.

In addition to a 6 KV power supply, preamplifier,amplifier-discriminator, scaler, timer, and linear/log counting-rate meter, a home-built reset, event-marking programmer, Figs. 12 and 13, was needed.

Interpreting the output of a scaler used in conjunction with gas chromatographic analysis can be a serious problem. One possible method is to record the output of the scaler at fixed time intervals, but this involves either a tedious manual recording procedure or an expensive printer, and requires subsequent replotting of the data in either case to determine peak location and magnitude. Another solution is to feed the output of the scaler into a counting rate meter and follow the output of the meter on a pen recorder. This defines the peaks nicely, but requires integrating a curve which is anything but smooth. This latter method can compound errors. The data are available initially as counts; the counting rate meter indicates the derivative of the original data; by finding the area under the curve the "integral" is determined and, in effect, the initial data, counts, recalculated.

We have devised a system which provides data in a convenient non-cyclic form without the expense of a digital integrator or printer. The output of the amplifier/discriminator is fed into a counting rate meter and then to one pen of the recorder (the other reads thermal conductivity). In addition, a signal originating in the scaler after a preset number of counts is used to trigger an event marking pen on the same recorder thus affording simultaneous representation of

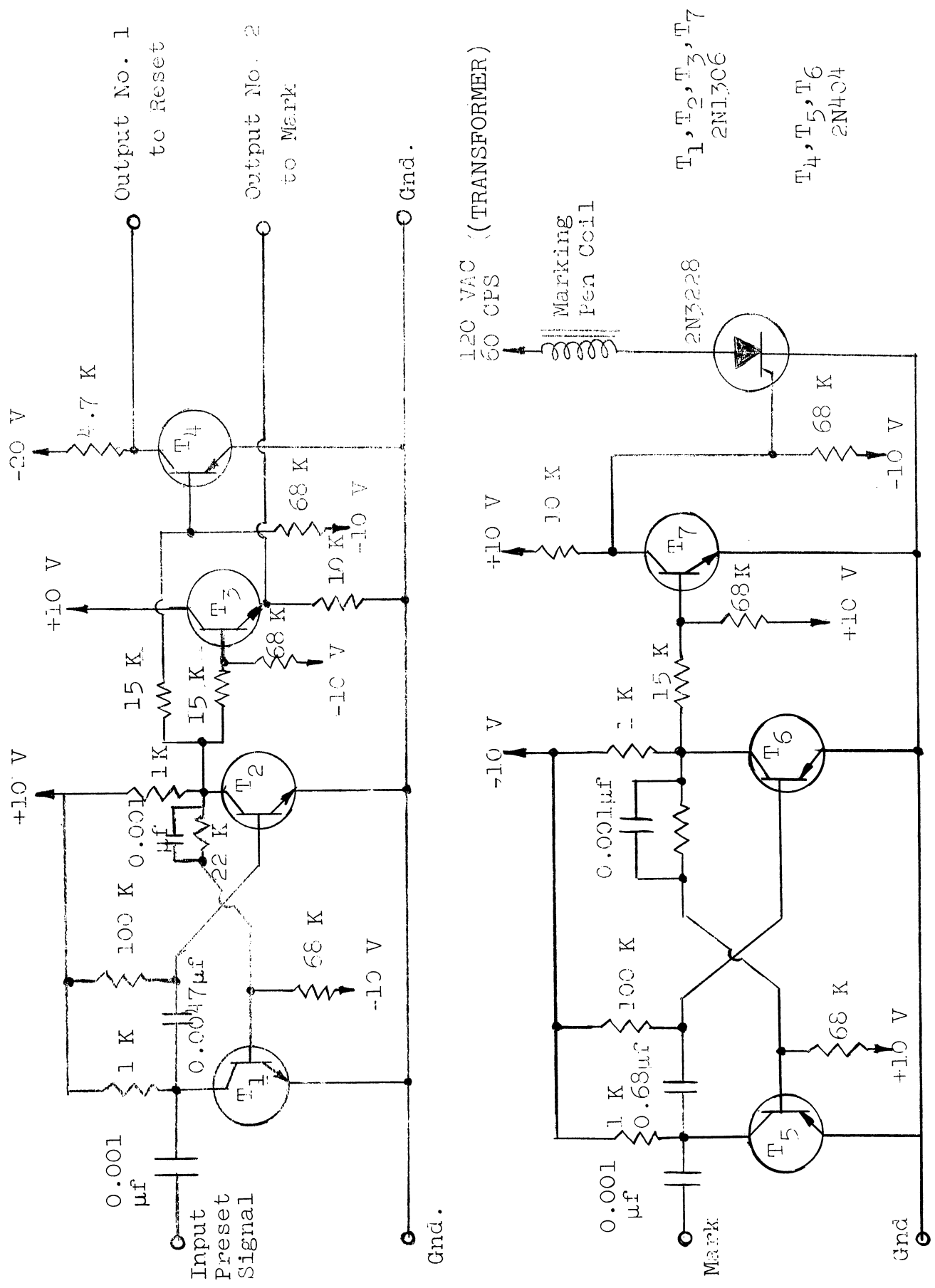

Figure 13. Circuit for reset, event marking programmer.

thermal conductivity data, counting rate, and total activity on the same time base.

The trigger circuit takes a - 10V signal from the scaler occurring when a present condition is reached, at which time the scaler stops counting until a suitable pulse is fed into the reset line, to trigger a monostable which generates a 35 μs reset signal. This is sufficient time for the scaler to reset all circuits without introducing an appreciable dead time into the counting circuit. Should it ever become necessary, knowing the counting rate at the time such a reset occurred, it is a simple matter to introduce an appropriate "reset-time" correction factor. The same signal triggers a 50 ms mono-stable which feeds a signal to the gate of a silicon controlled rectifier in the marking per circuit. Each time the scaler reaches a preset condition, which can be either a fixed number of counts or a time interval, as selected by various controls on the front panel of the instrument, a mark appears on the chart. The activity of the peak is the number of marks occurring under the area defined by the counting rate meter multiplied by the scaling factor.

Our unit is entirely solid state and is built on the same boards as the RIDL electronics. Exclusive of the case, it could be duplicated for about $40, and consists entirely of readily available components.

The advantages of this method are:

1) the data all appear on one chart in a form which is easily interpreted without replotting, Fig. 14, and

2) the associated circuitry does not involve the expense

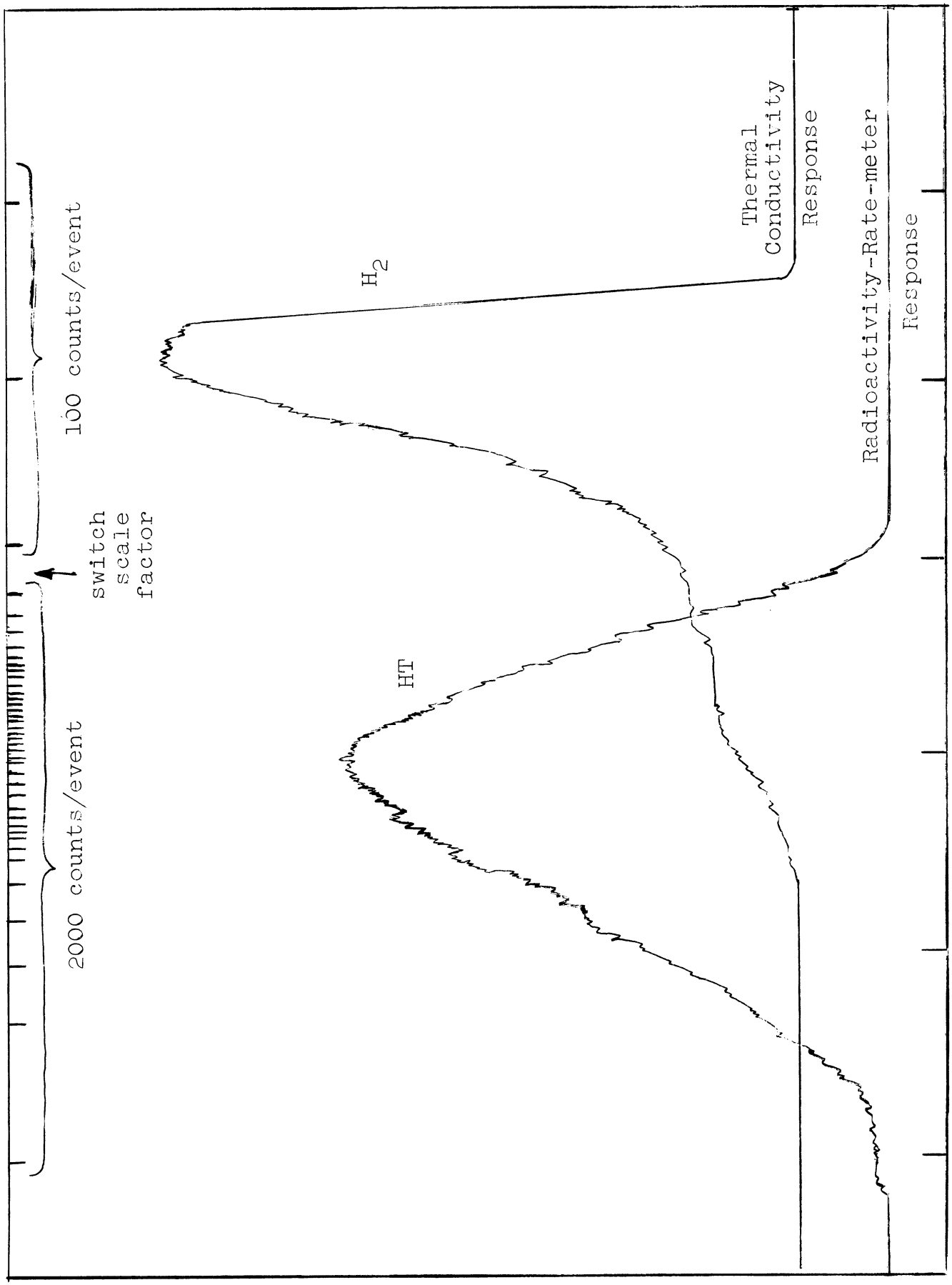

Figure 14. Typical recording of tritium chromatography peak and scaler event markings.

of digital integrators or printers as used by other groups for this purpose.

With the RIDL equipment there is considerable versatility possible in selecting ranges, and variations on the idea can be adapted to almost any scaler. For example, the pulse which triggers a mechanical counter can be used to operate the pen through a plate relay. We find this most satisfactory with our Nuclear-Chicago Ultra-Scaler as used in the strong-beta detecting gas chromatograph described in the previous section.

The flow proportional counter, Fig. 15, is a practical device for detecting weak-beta emitters in gas chromatographic analysis, but the standard design consisting of a glass tube with silver cathode has many disadvantages. It is fragile, attacked chemically, cannot be cleaned, and cannot be taken apart easily to replace a broken or sagging anode. Furthermore, it is almost impossible to determine the condition of the anode unless it is actually shorted to the cathode.

Schmidt-Bleek and Rowland, [Analytical Chemistry, 36, 1675 (1964)] have proposed a design for a brass teflon counter which can be taken apart easily and cleaned, has variable volume determined by the length of the cathode section employed and has excellent counting characteristics (discussed in detail below). It is rugged, and the anode is easily replaced if necessary. The background is low, even without additional shielding. Total cost for the unit is about $100. Basically the tube is a brass cylinder threaded with teflon end pieces which hold the anode and double as high voltage insulators.

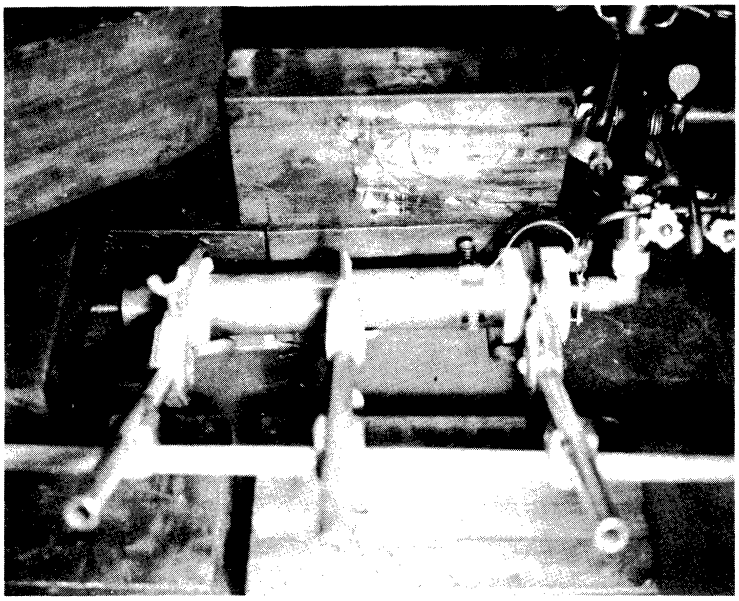

Figure 15. Flow proportional counter.

The brass center section is readily changed and can be made in a wide range of volumes to suit particular considerations of specific activities and column resolution. At present we are using a cathode section with 40 cc volume, but plan to test other volumes in the future.

We have determined counting characteristics of the tube over a wide range of helium-propane mixtures and flow rates. Some results of these determinations are reported in Fig. 16. It is apparent that the plateau for a 1:1 helium to propane mixture is about 700 volts long and has a slope of about 0.2%. Moreover, it is relatively insensitive to fluctuations in the composition of the counting mixture. This is most important in gas chromatographic work since the composition of the mixture changes during the passage of a macro-sized sample through the counter. We have not been able to detect a significant change in counting characteristics during the passage of air and hydrogen samples.

The only points of construction deserving special note are

1) the interior of the cathode section must be carefully polished to avoid discharge and
2) the anode wire must be free of kinks and surface imperfections.

Currently we are using 0.005" No. 302 stainless steel wire for the anode. It seems to perform satisfactorily and is much easier to work with than tungsten.

(R. Pearson, Jr.)

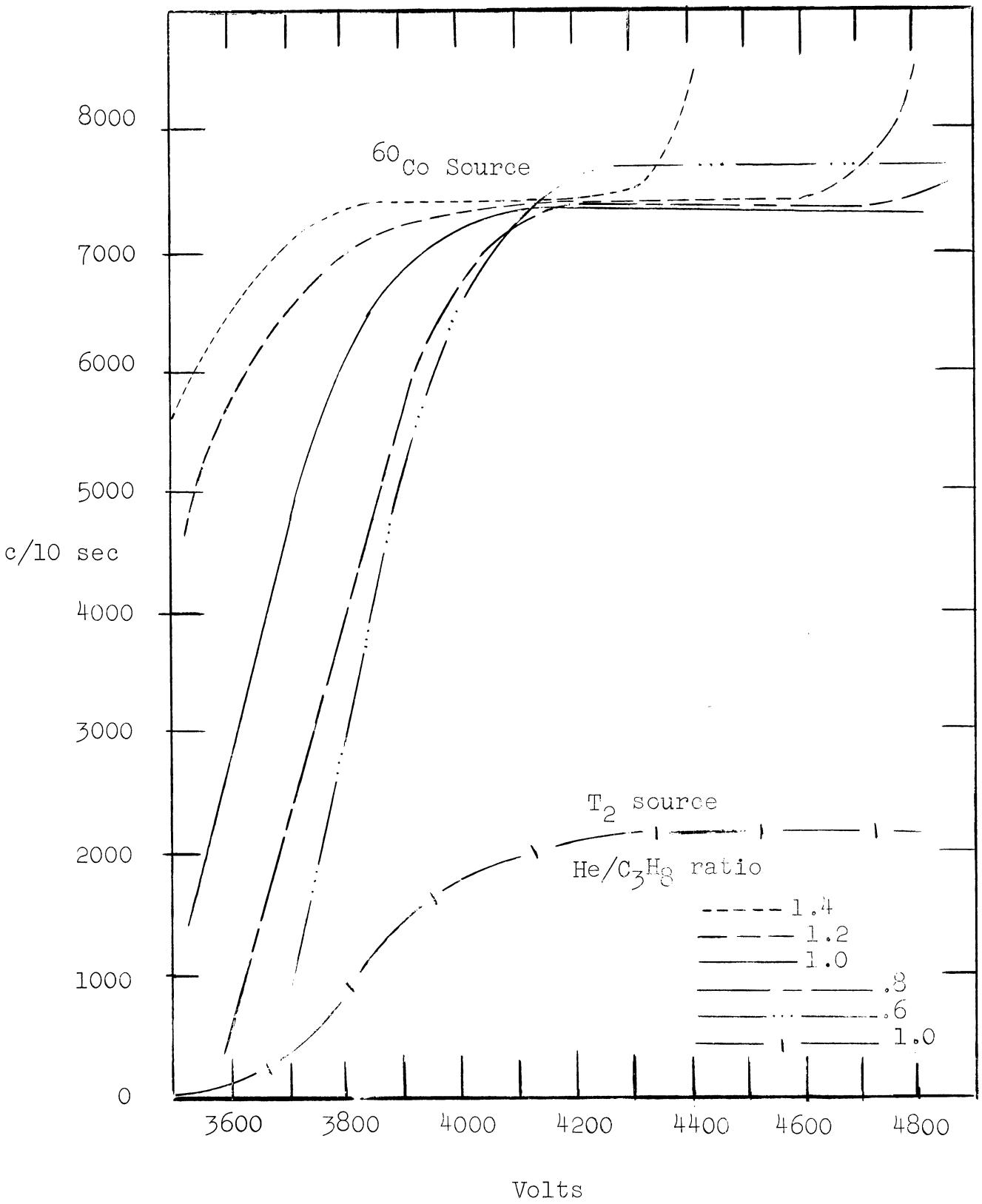

Figure 16. Plateaus for flow proportional counter, upper curves using a ^{60}Co source, lower curve using T_2 in non-flow counting.

4. Two Channel Radio Gas-Chromatograph

Some of our hot-atom studies involve the production of two radioisotopes, For example, irradiation of $CHCl_3$-I_2 mixtures results in both ^{38}Cl (37.5 min., 1.64 MeV gamma) and ^{128}I (25 min., 0.45 MeV gamma) . Certain products such as CCl_3I may, in some molecules contain ^{38}Cl and in others contain^{128}I. Routine radio-gas chromatographic analyses of such systems could be easily performed using a two-channel radio-gas chromatograph. We have borrowed equipment to construct temporarily a unit as diagrammed in Fig. 17, and plan to buy the necessary components in the near future.

(A. Gordus)

5. Photochemical Studies Vacuum Line

Shown in Fig. 18 is a block diagram and in Fig. 19 a photo-graph of the vacuum line used in photochemical hot-atom studies. The line used in the sample preparation is kept mercury-free (Traps T_1, T_2, T_3, T_4, T_6, and T_7 in Fig. 18) in order to prevent chemical decomposition of hydrogen bromide, and a quartz spiral gauge is used for pressure measurements. Because many non-condensible gases were used the volume of the vacuum line was kept to a minimum.

Various preliminary "dark" runs indicated that appreciable amounts of the hydrogen bromide samples were being decomposed. Part of the decomposition was due to the fluorescent lights in the room; small wattage incandescent bulbs are now used. Additional decomposition was due to > mg amounts of mercury contamination of the sample section as detected by neutron

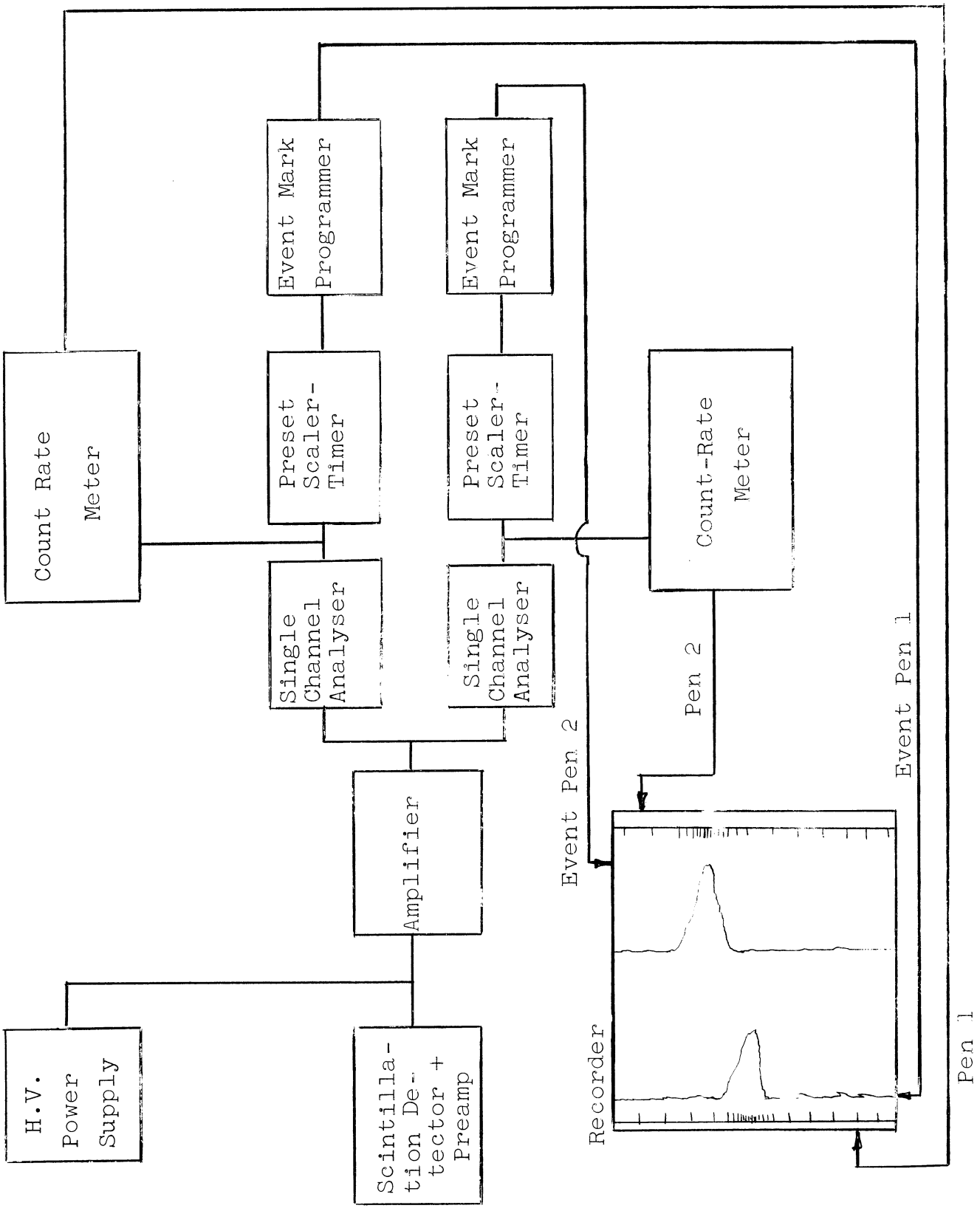

Figure 17. Block diagram of two-channel gamma-detecting radio-gas chromatograph.

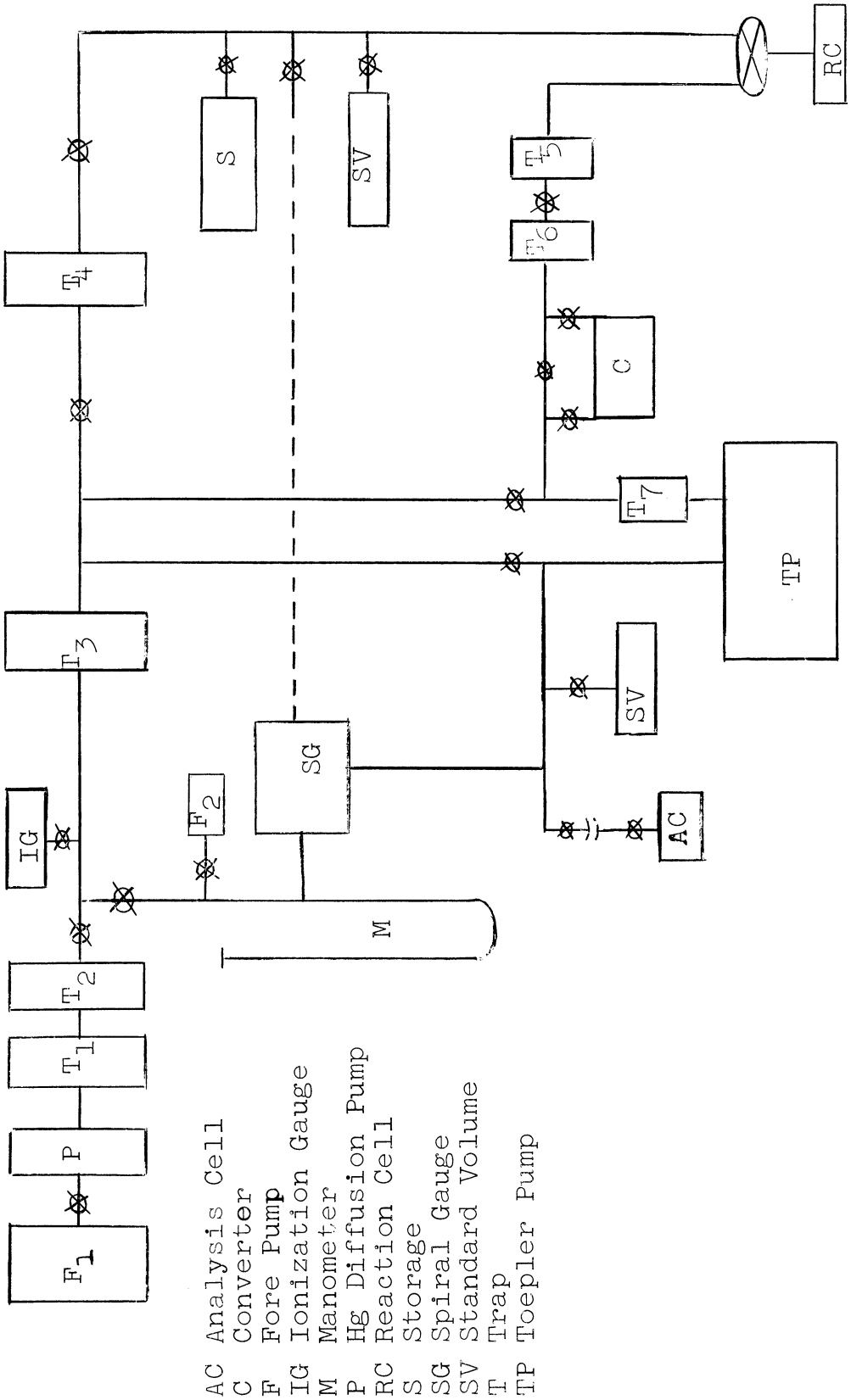

Figure 18. Block diagram of vacuum line for use in photochemical hot-atom reaction studies.

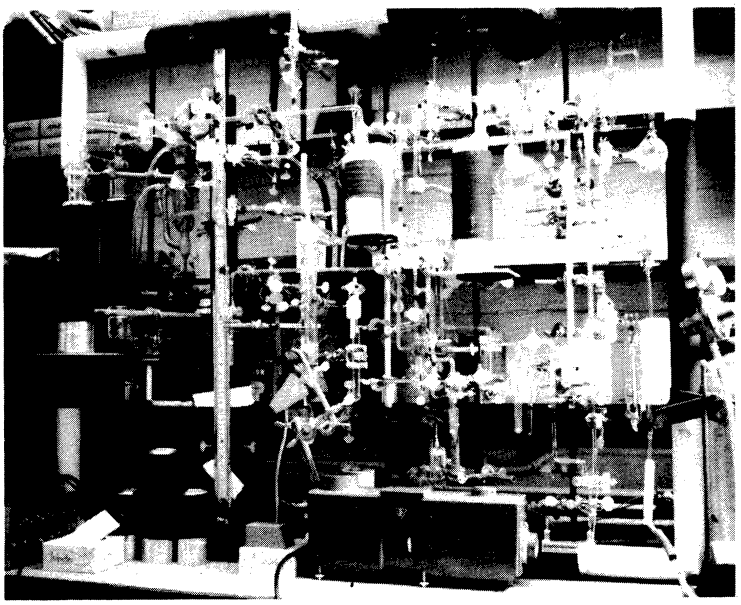

Figure 19. Vacuum line diagrammed in Fig. 18.

activation analysis of glass wool packing originally in trap T_5, when trap T_6 was not present. The present arrangements of traps, (Fig. 18) was designed to overcome this problem.

A Bausch and Lomb monochromator with a diffraction grating blazed at 2000Å is used as the source of UV photons. A calibration of the monochromator output using a calibrated Beckmann DU spectrophotometer is shown in Fig. 20. As seen, corrections arise only below 2300Å, although the error may be due in part to the unreliability of the Beckmann DU at wavelengths approaching 2000Å . For higher wavelengths, the monochromator peak output for a given wavelength setting appears to be about 10 to 15 Å below the Beckmann DU peak intensity reading. This is an error of less than 0.5%.

(J. Griffith)

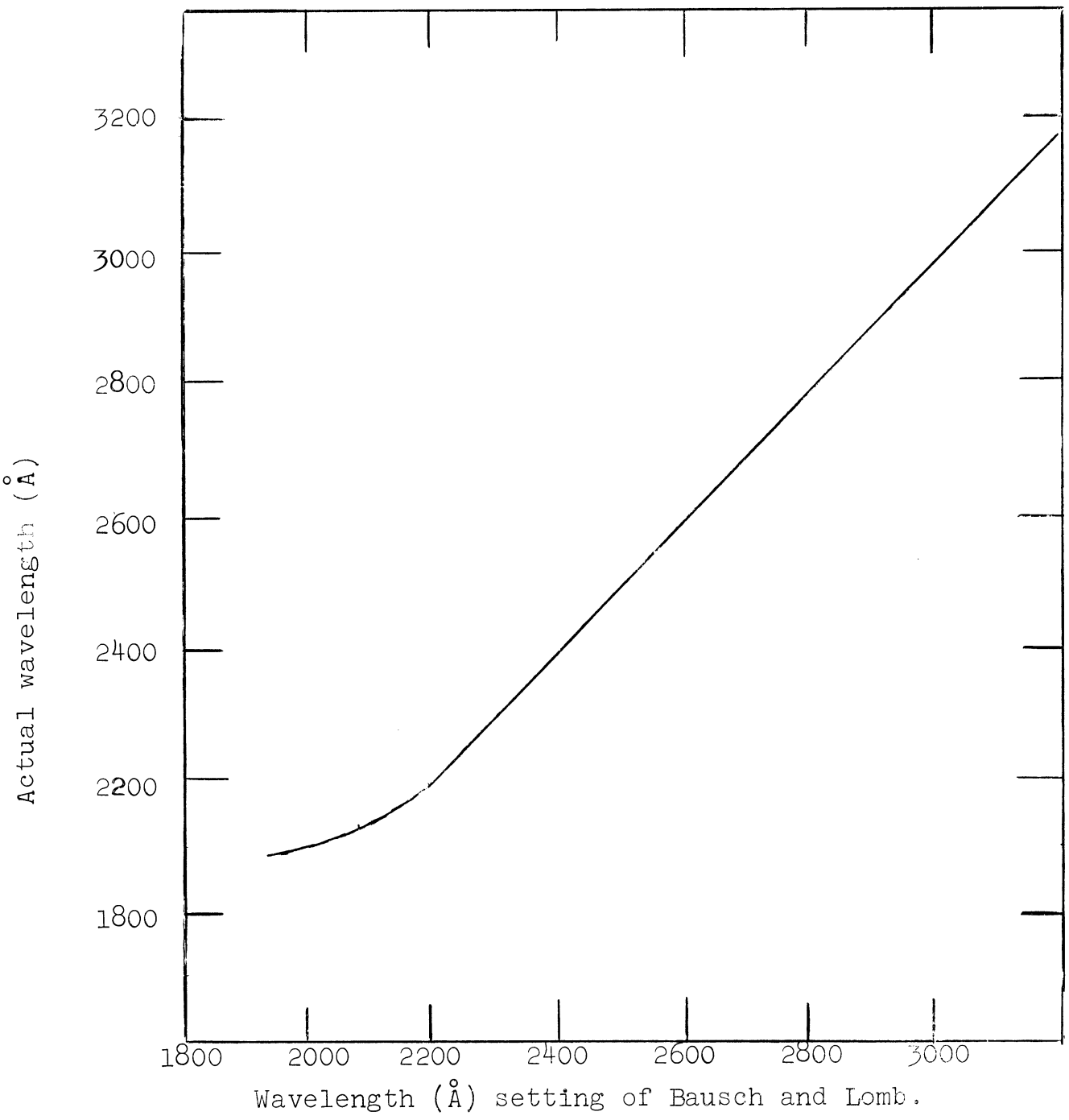

Figure 20. Monochromator wavelength reading versus actual wavelength.

III. EXPERIMENTAL AND THEORETICAL RESULTS

1. Gas Chromatographic Separation of Isotopes

As noted in the 1964 Progress report, we have obtained a separation of macro-amounts (5 cc-atm) of CH_4-CD_4, Fig. 21, in about 70 minutes. It should be emphasized that macro isotopic separations are much more difficult than separations of smaller-sized (e.g. 0.1 cc-atm) mixtures of isotopically-labeled substances since these latter separations can be achieved using highly efficient capillary gas chromatographic columns. For the analytical detection of stable-isotope labeled molecules the capillary method is satisfactory. However, we anticipate, for example, the need to determine the relative amounts of CH_3T and CD_3T present in a CH_4-CD_4 mixture, and only with sample sizes of the order of 5 cc atm would sufficient tritium activity be present to permit accurate measurements of the CH_3T-CD_3T contents. In addition, the development of macro separation techniques could be useful in devising methods of preparation of isotopically-enriched compounds.

As shown in Fig. 22, separation of 5 cc-atm amounts of C_2H_6-CH_3CD_3-C_2D_6 has also been achieved.

Currently being investigated is the separation of CH_3T-CD_3T in CH_4-CD_4 mixtures as well as C_2H_5T-CH_2TCD_3-CH_3CD_2T-C_2D_5T in the ethane mixtures. Since the protonated-deuterated compound separations have been shown to be possible, the separation of the tritiated species will also be possible.

Another study involves the ^{12}C-^{13}C separation. For isotope-ratio mass-spectral analysis the carbon is usually in the form

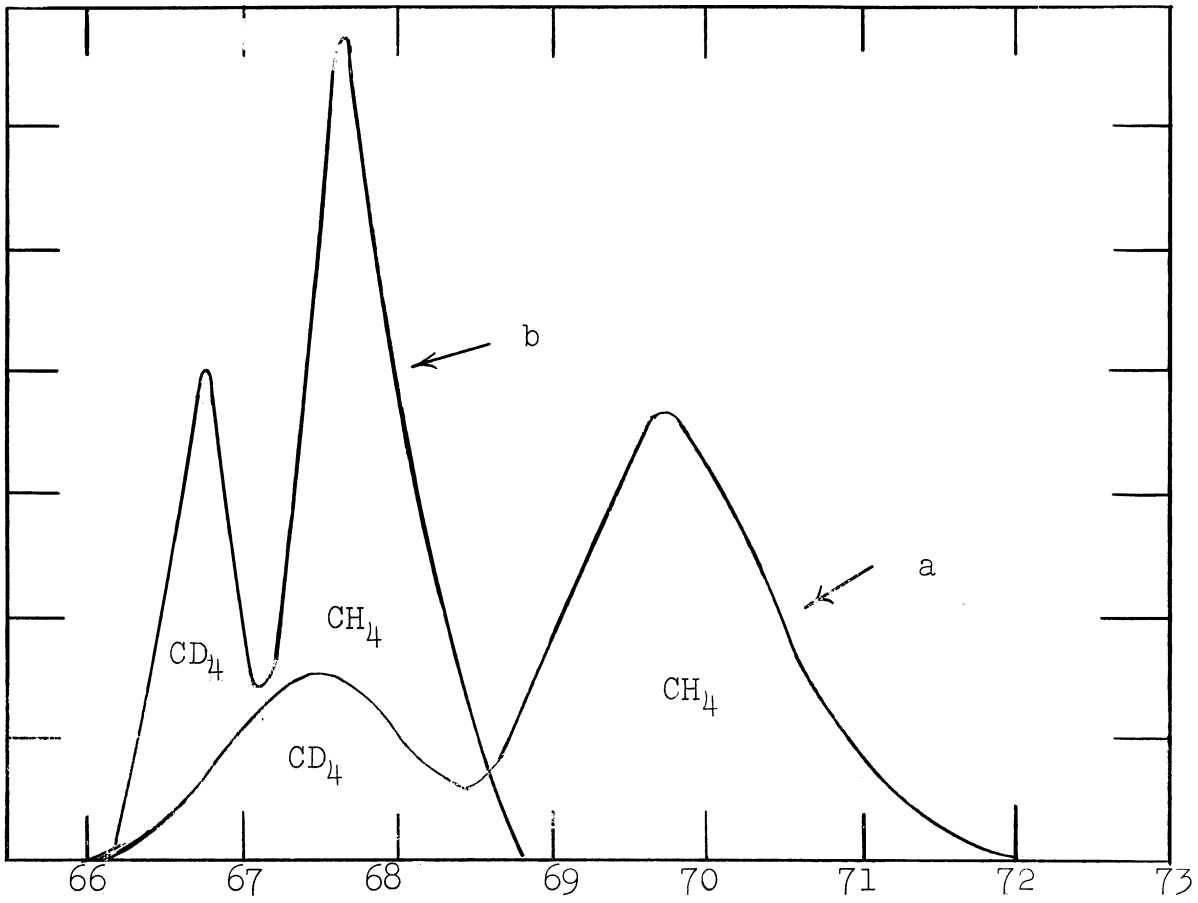

Figure 21. Our separation of a CH_4-CD_4 gas mixture using a 45', 1/4" copper tubing of column packed with 15 ft. of 40/60 and 30 ft. of 60/80 mesh 13X Molecular Sieve. Operated at -15°C. Curve a, 145 cc/min He flow. Curve b, 91 cc/min He flow with column heated just prior to emergence of the CD_4 peak.

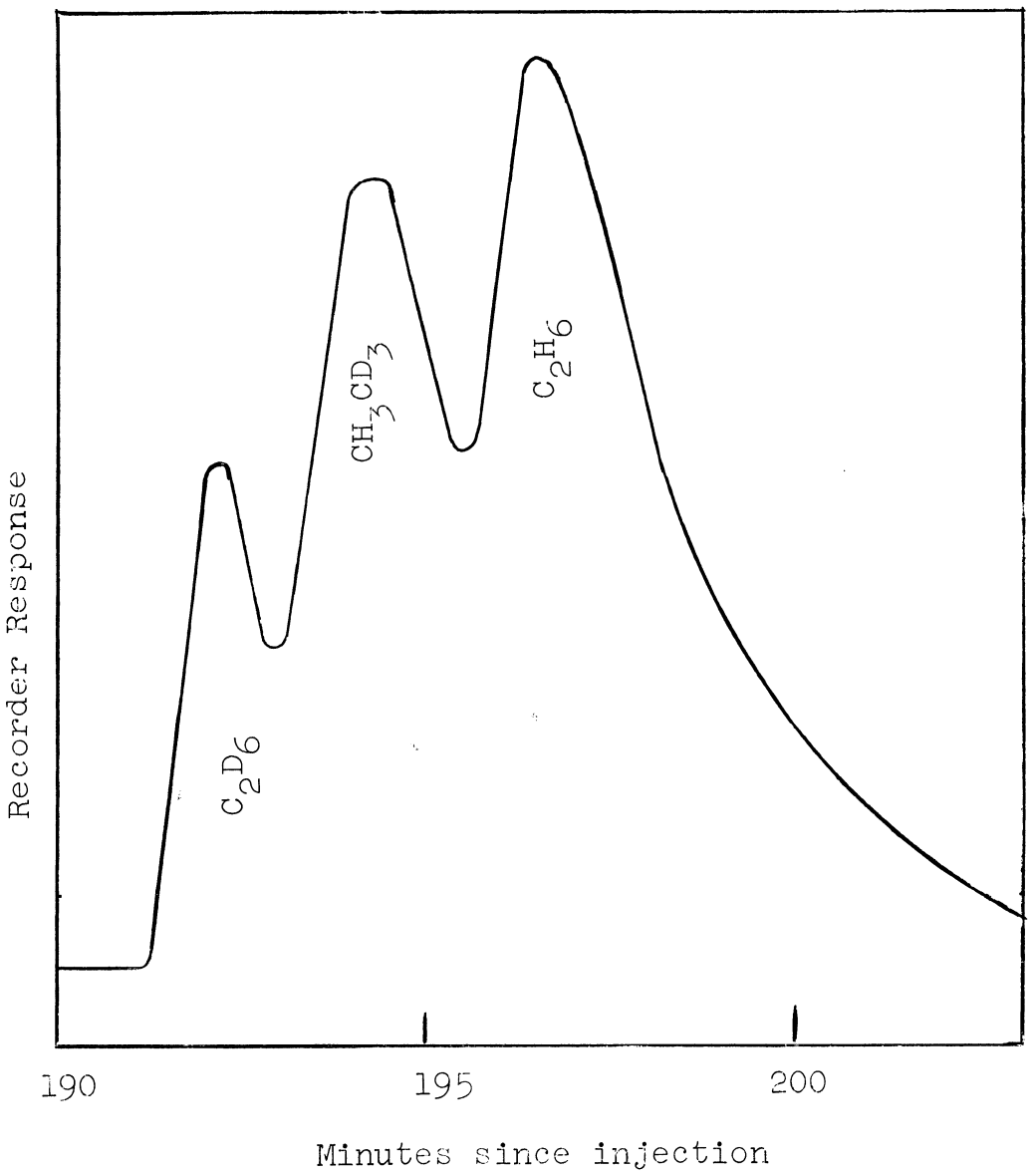

Figure 22. Gas chromatographic separation of C_2H_6-CH_3CD_3-C_2D_6.

of CO_2. However, we anticipate that a better separation will be possible if we can operate the chromatography column at liquid nitrogen temperature (-196°C). CO_2, of course, has a very low vapor pressure at this low temperature. Hence, we have built a pre-column reduction unit (Fig. 1) to permit CO_2 to CO conversion prior to the gas chromatographic separation. Data on the feasibility of ^{12}CO-^{13}CO separation are not yet available.

Additional separations to be investigated include $^{14}N^{14}N$ - $^{14}N^{15}N$ and $^{14}NH_3$-$^{15}NH_3$. Methods of enriching the ^{48}Ca content of natural calcium are also being evaluated.

(W. Litzenberg)

2. UV Absorption Spectra of Isotopic Hydrogen Halides

The only published data on the continuous ultraviolet absorption spectra of DI or DBr are those of Bates, Halford, and Anderson [J. Chem. Phys., 3, 415, 531 (1935)]. We have determined the absorption spectra of gaseous HI, DI, HBr, and DBr over the wavelengths 2100-3200 Å, at 20 Å intervals. For HI and DI up to 60 separate determinations were made at certain wavelengths. For the HBr and DBr preliminary study only 5 to 10 determinations were made at each wavelength. Using a computer program devised by a Sophomore Honors student (G.W. Moore) absorption coefficient data for a given wavelength were averaged, standard deviations determined, data falling outside the error range as given by Chauvenet's criterion were rejected, and new averages and standard deviations calculated and the process repeated. Figure 23 is a typical computer output for HBr absorption data at 2440 Å. Printed out are λ, ν, $\tilde{\nu}$, ϵ, log ϵ, log $(\epsilon/\tilde{\nu})$, log(ϵ/ν), σ_ϵ, $\sigma_{\bar{\epsilon}}$, the Student t-95% confidence level

LAMBDA	NUBAR	NU	EPSILON	LOGEPS	LOGEPS/NUBAR	LOGEPS/NU	SIGEPS	SIGEPSBAR	95CONFLIM	N
2440.0	4.09836E 04	1.22866E 15	4.079	.61053	.99792	1.52110	.1095	.03870	.09153	8

USED DATA

4.1200 4.2300 4.1700 4.0900 4.1200 4.0000 3.8800 4.0200

REJECTED DATA

Figure 23. Computer output for data rejection and standard deviation calculations of spectral absorption measurements.

$\sigma_{\bar{\epsilon}}$, and the number of data used in the final computation.

In Fig. 24 are solid-line plots of our data for log ϵ for HI and DI. Data of Bates, Halford, and Anderson are also shown. As seen from the solid lines the curve for DI is shifted to higher energies (wave numbers). This results from the lower vibrational energy of DI; hence, more energy is needed for the DI to undergo a transition from the DI lower vibrational energy state to the upper repulsive energy curve. The DI maximum absorption coefficient is greater than that of HI since the ground state DI eigenfunction is compressed relative to the HI eigenfunction; hence the maximum in the DI eigenfunction is larger than that of HI.

Of particular interest is Fig. 25. Rather than a relatively smooth function a "sine form" is suggested in the region of 34-38,000 cm^{-1}. At first an impurity in either the synthesized HI or DI was thought to be the cause. This was not the case. Apparently in these compounds, absorption of UV radiation can sometimes lead to a transition to a repulsive state involving ground state iodine. Other absorptions may lead to electronically excited iodine. This is illustrated in Fig. 26 by the transitions A and B, respectively. These two transitions would result in two absorption curves, Fig. 27, and the composite curve would be observed experimentally. The isotopic molecule (DI) would also exhibit a similar composite curve; when the ϵ ratio is plotted, as in Fig. 25, a sine-form curve should result since the isotopic shift of curve A, Fig. 26, would, in an ϵ ratio calculation, first enhance, then suppress the presence of transition A.

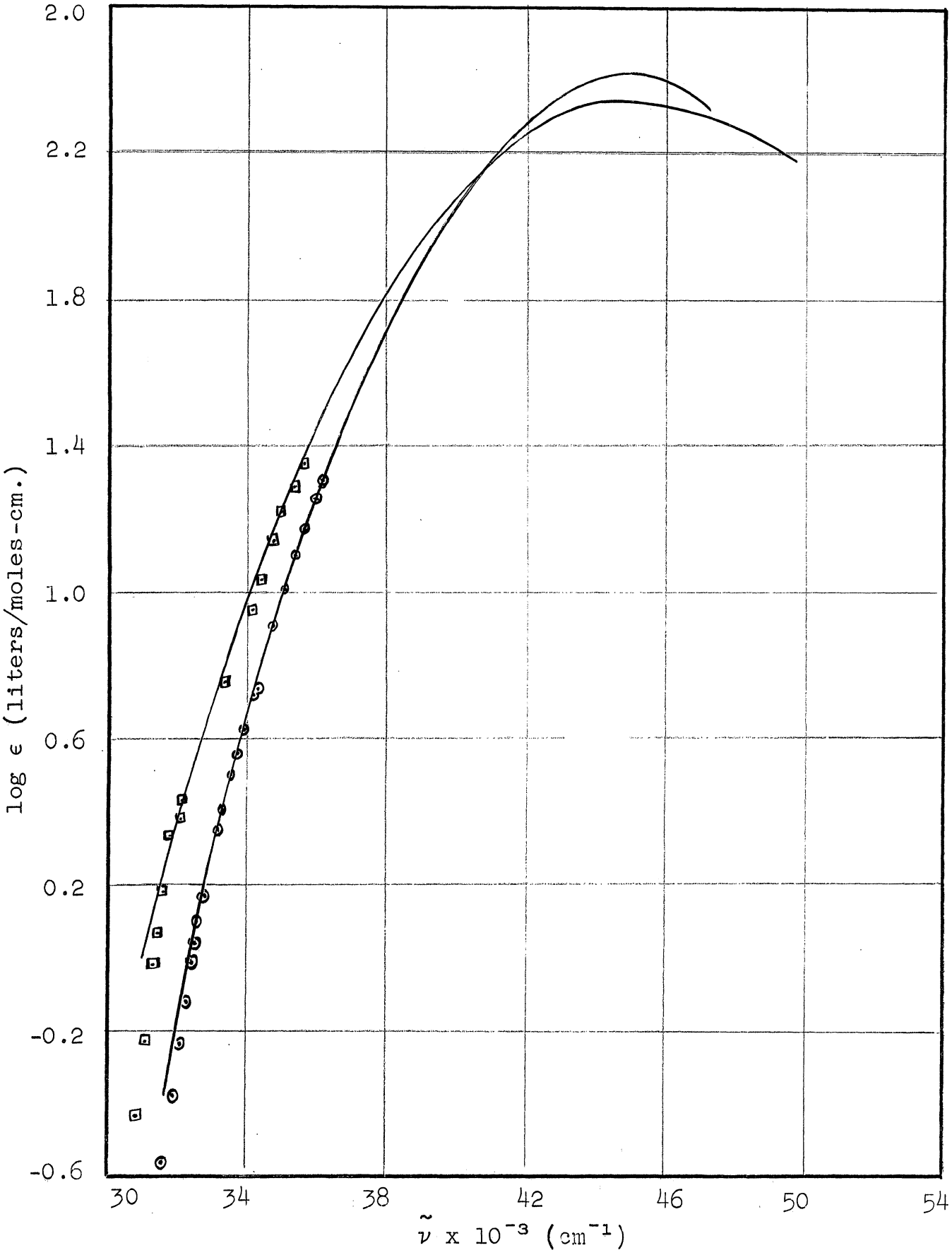

Fig. 24. Ultraviolet absorption spectra of gaseous HI and DI. Solid lines are the best fit through present data. Data of Bates, Halford, and Anderson, [J. Chem. Phys. 3, 415 (1935)], ⊡ , HI; ⊙ , DI.

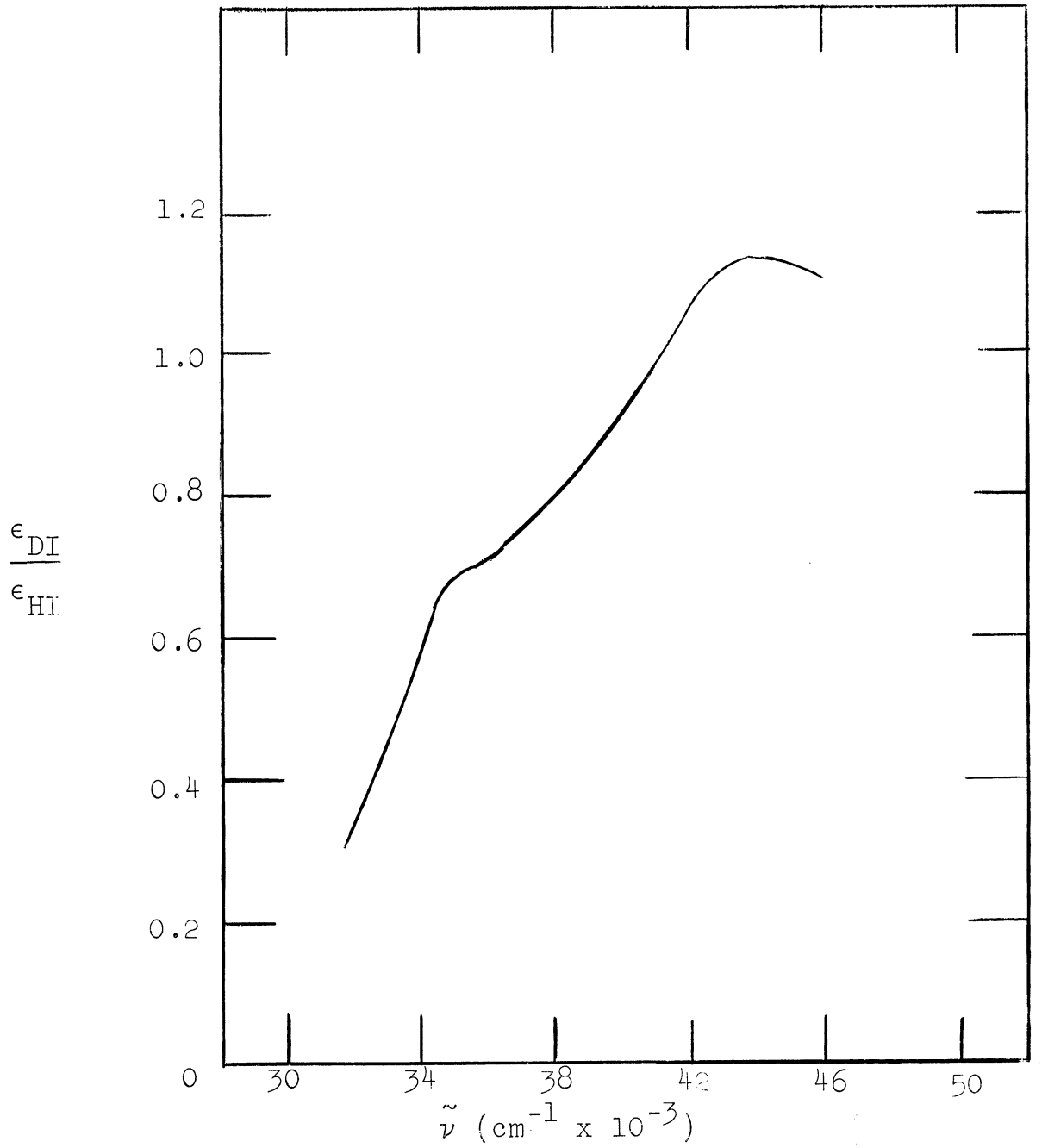

Figure 25. $\epsilon_{DI}/\epsilon_{HI}$ versus $\tilde{\nu}$.

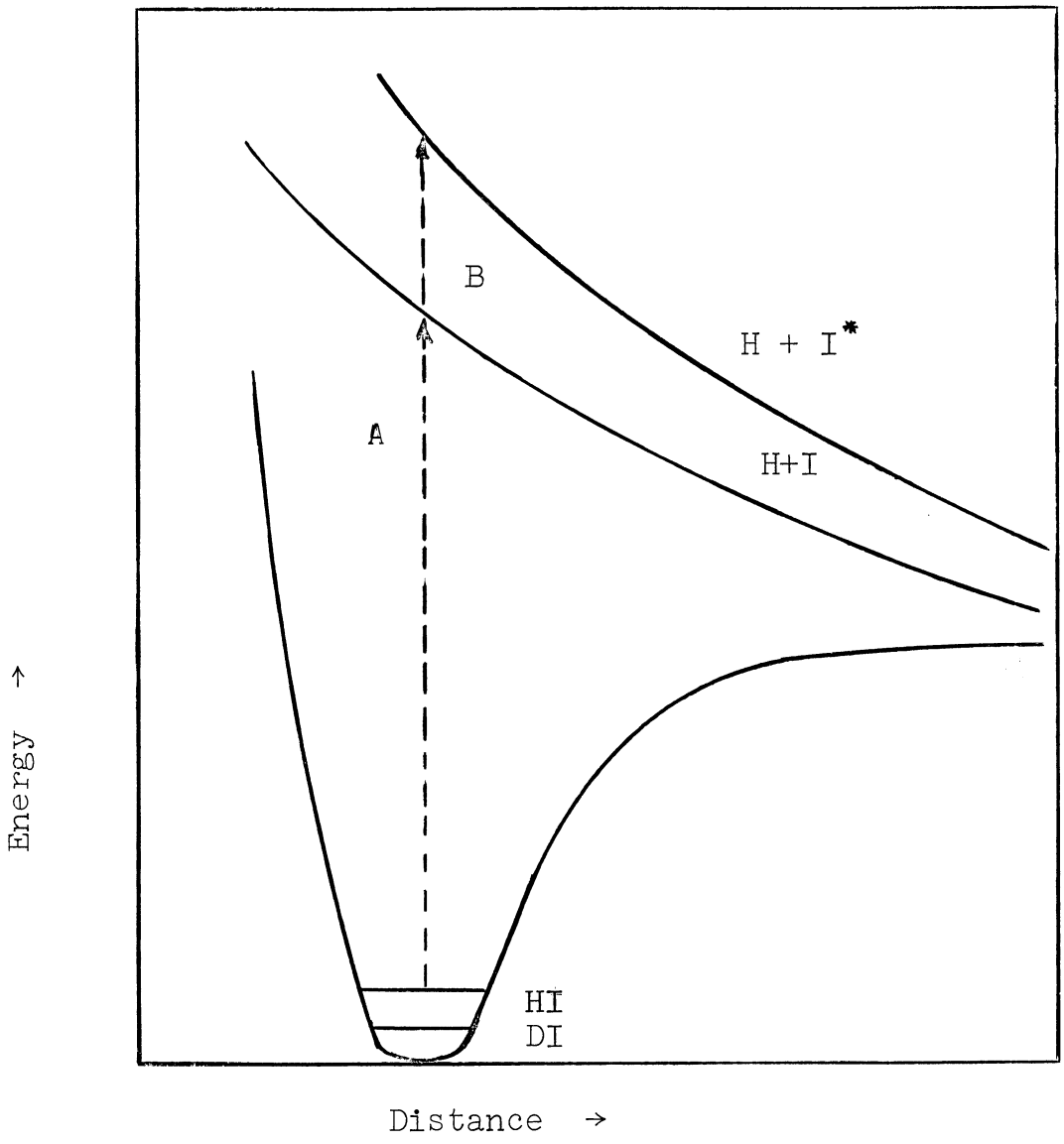

Figure 26. Absorption to two repulsive states.

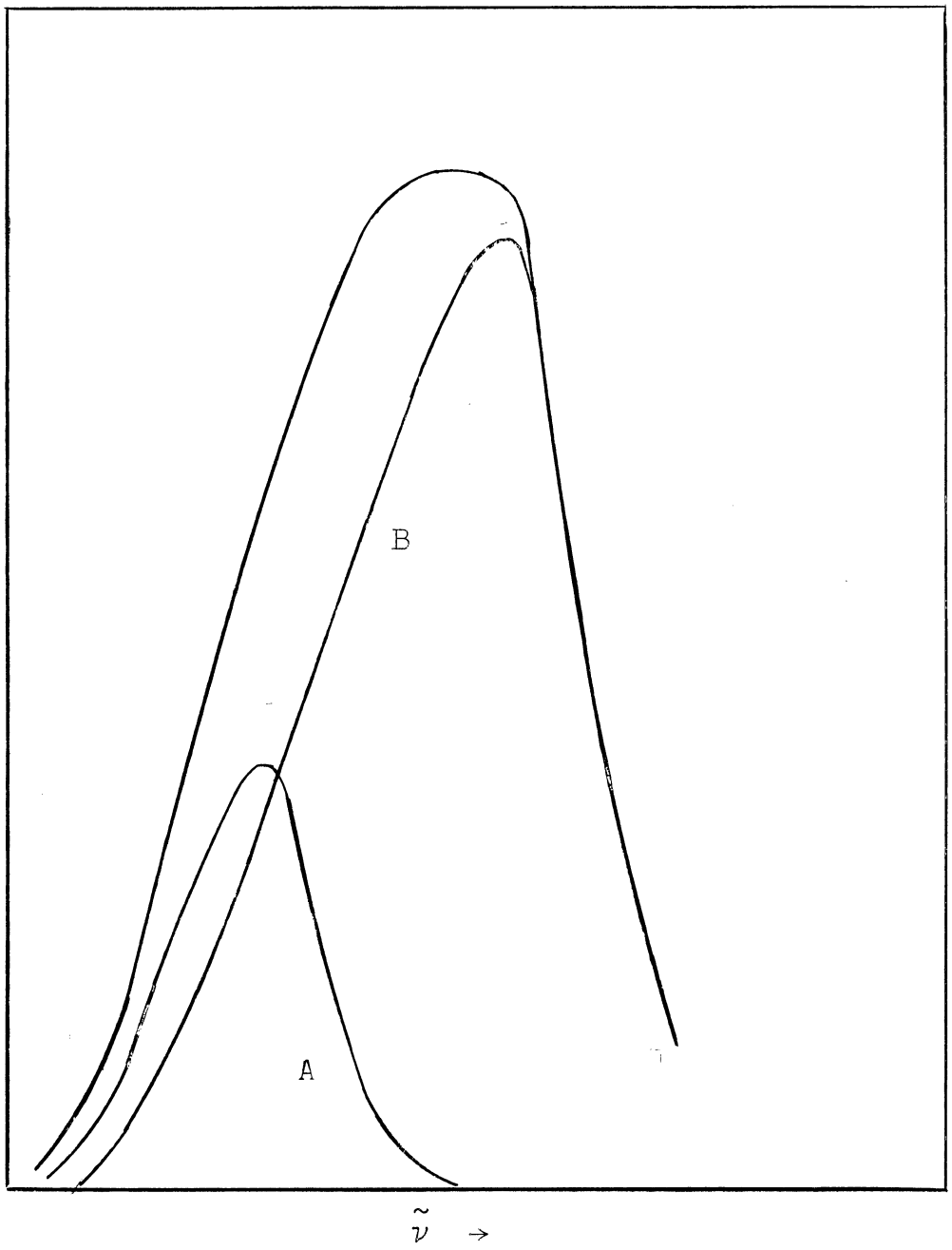

Figure 27. Hypothetical composite absorption curves for hydrogen iodide

We have approximated this effect using mathematically synthesized data of the type sketched in Fig. 27.

Currently we are examining these data in order to be able to determine the type A (ground-state iodine) absorption maximum. In addition, we are attempting to predict theoretically the TI curve prior to measurement.

Figures 28 and 29 are for HBr and DBr. As seen in Fig. 29 a smooth ϵ-ratio function results. This is not unexpected since transitions to produce excited Br are much less likely than are excited I in the HI-DI spectra.

(D. Caughey)

3. Photochemical Hot-Atom Reactions

As noted in the preceding section, absorption of ultraviolet light by HBr, DBr, or TBr leads to a transition to a repulsive state which is followed by dissociation of the diatomic molecule. Any energy in excess of the bond-dissociation energy is released as translational kinetic energy of the two atoms. From conservation of momentum and energy requirements it can be shown that the hydrogen atom will possess $80/(80 + m_H)$ of the energy in excess of the bond dissociation energy. Figure 30 is a plot of the hydrogen energy as a function of the wavelength of the absorbed radiation.

As seen in Fig. 30, H, D, or T atoms with initial energies up to 3 eV (i.e. 36,000 °K) can be produced. If these high-energy atoms are generated in the presence of a gas which is at thermal energy (0.025 eV, 300°K) hot-atom reactions could occur. If the initial energy of the hot hydrogen atom is increased in a set of experiments it is possible to determine

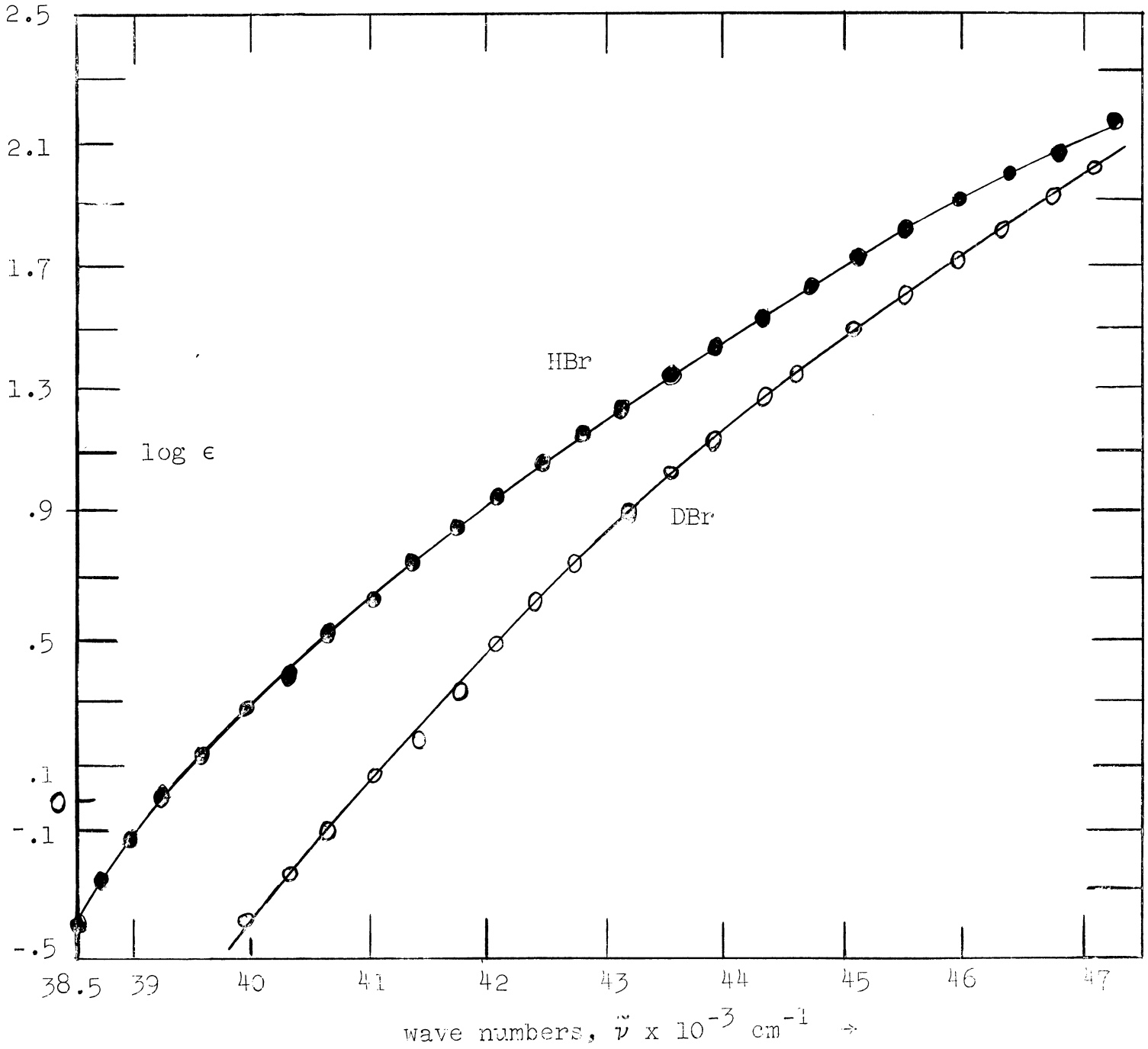

Figure 28. log ϵ_{HBr} and log ϵ_{DBr} versus $\tilde{\nu}$.

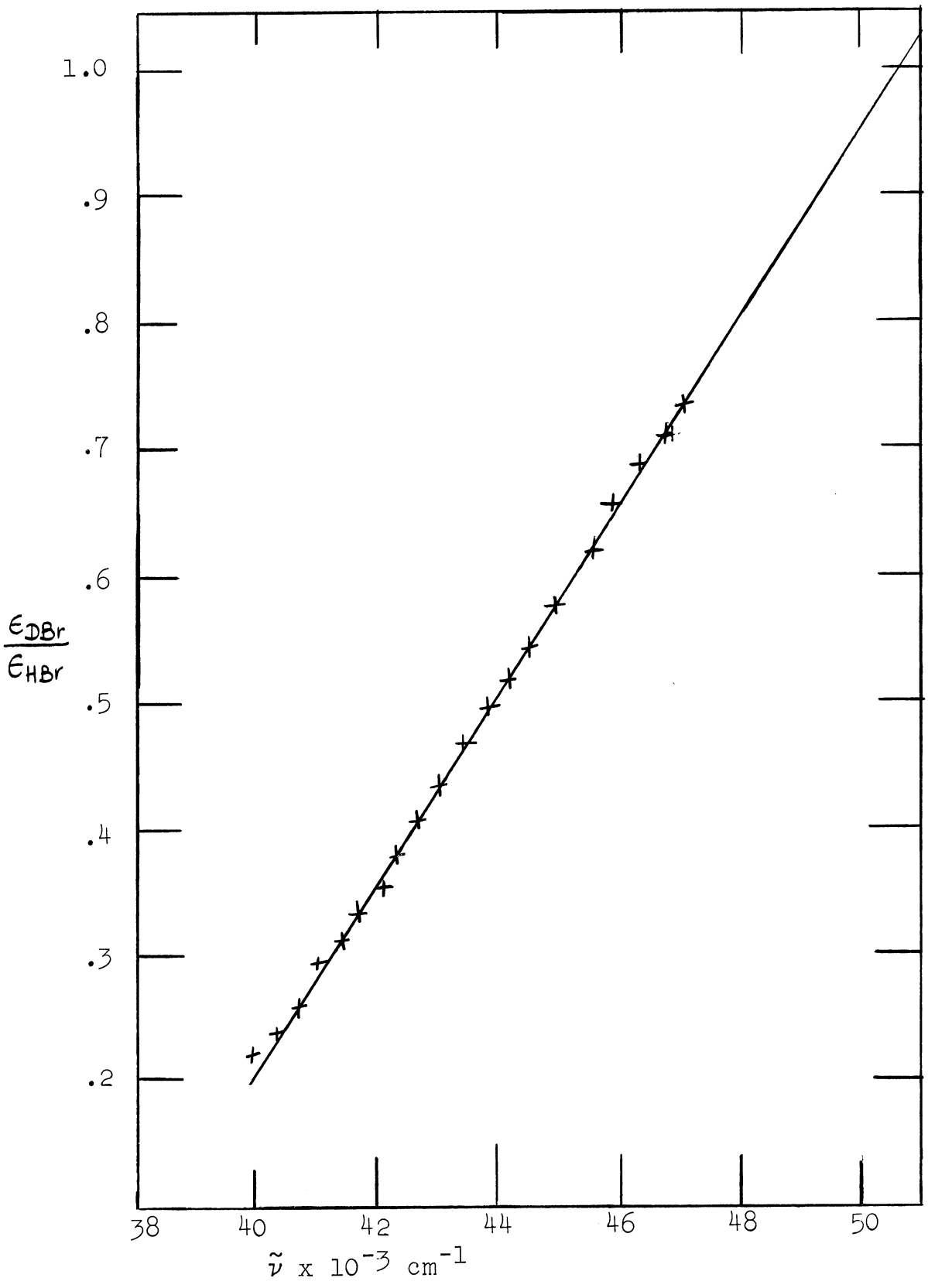

Figure 29. $\epsilon_{DBr}/\epsilon_{HBr}$ versus $\tilde{\nu}$.

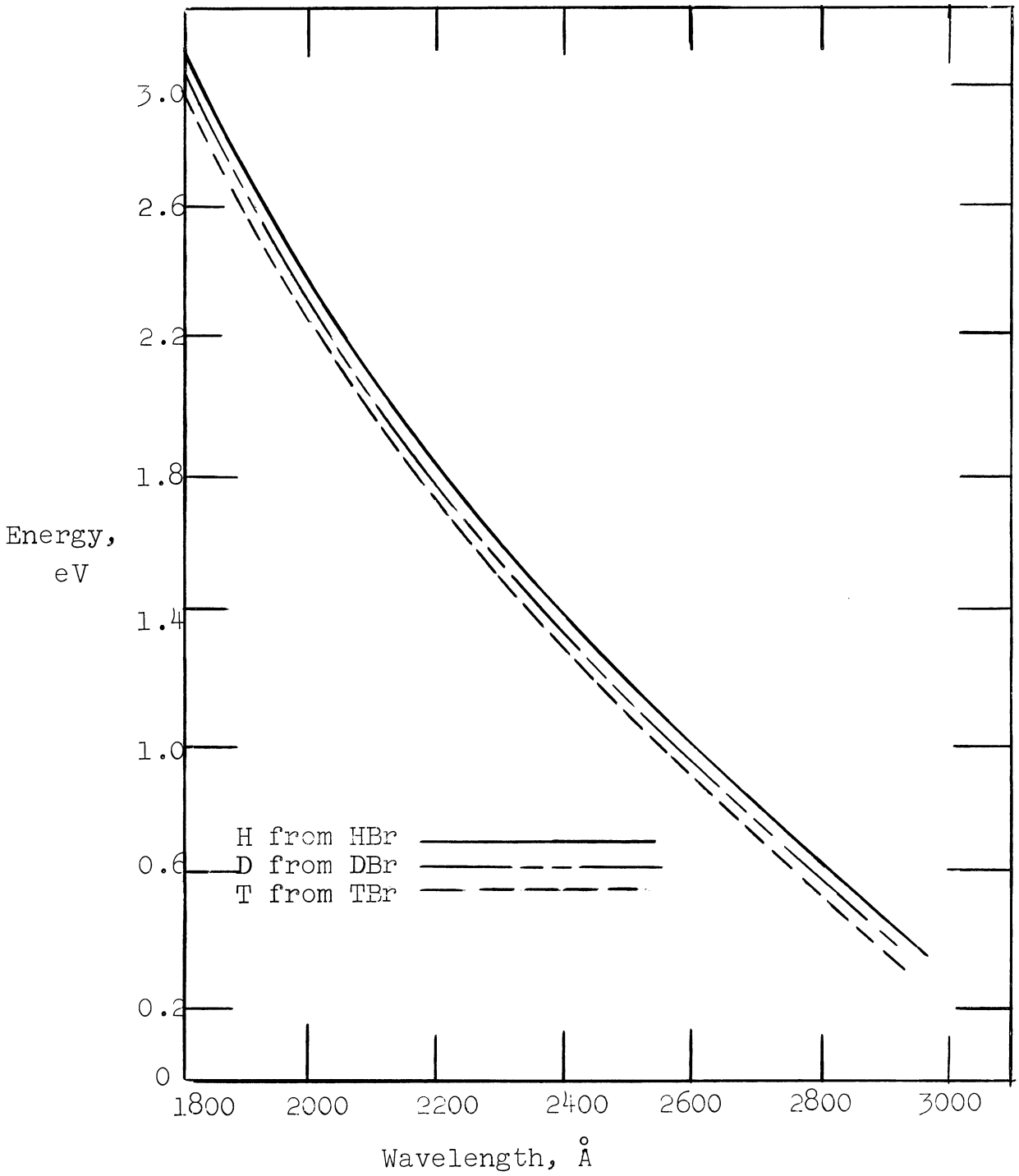

Figure 30. Hydrogen atom energy values versus λ.

the energy at which reaction begins. This energy threshold is related to the Arrhenius activation energy. By varying the composition of the mixture, using a reactive gas- He mixture, for example, it is possible to determine the variation of the extent of reaction as a function of the composition. These data would be useful in calculating such parameters as the relative collision cross-sections, the average collisional energy losses, and the reaction probabilities per collision.

(A. A. Gordus)

4. Reactions of (n,γ)-activated ^{80}Br with CH_4 and C_2H_6

Gas phase reactions of (n,γ) activated ^{80}Br with CH_4, CD_4, C_2H_6, and C_2D_6 have been studied as a function of the mole-fraction of the Br_2.

Figure 31 is a plot of the percent organic-^{80}Br formed in the reactions with CH_4 and CD_4. These data appear to describe two separate approximately parallel lines. We are not able to provide a simple explanation for the observation that the yield with CH_4 is about twice the yield with CD_4 (12.0 ± 1.0, 6.8 ± 0.8 %, respectively, at zero mole-fraction Br_2). Gas chromatographic analysis indicates two major organic products, CH_3Br and CH_2Br_2, or their deuterated analogs. In the $^{80}Br + CH_4$ reaction, 89% of the organic activity is due to $CH_3{}^{80}Br$. For the $^{80}Br + CD_4$ reaction, 76% of the organic activity is due to $CD_3{}^{80}Br$. Thus, at zero mole-fraction Br_2, 10.7% $CH_3{}^{80}Br$ and 1.3% $CH_2Br{}^{80}Br$ are formed compared with 4.9% $CD_3{}^{80}Br$ and 1.5% $CD_2Br{}^{80}Br$. We know of no simple

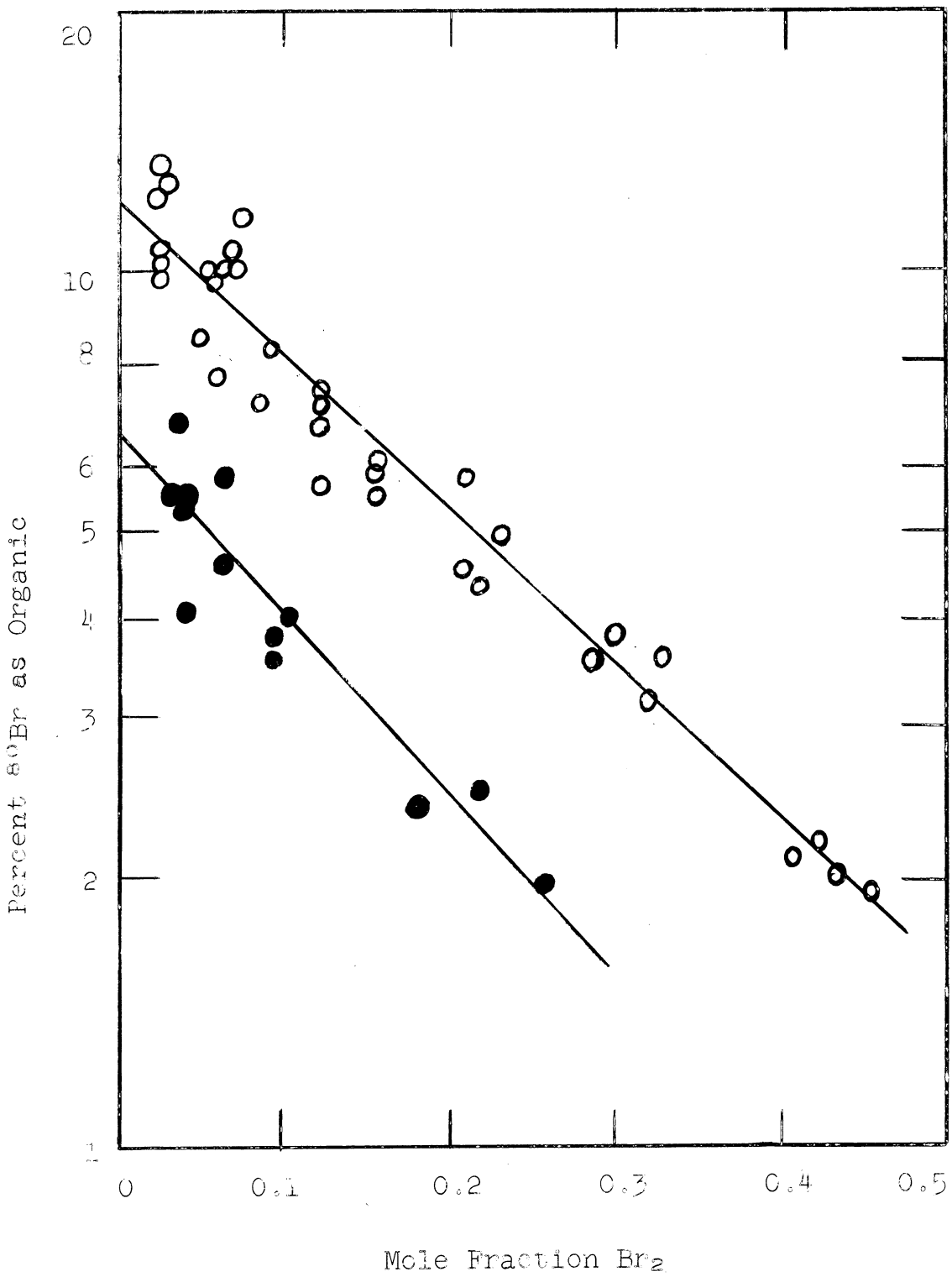

Fig. 31. Organic yields as a function of Br_2 concentration for $^{80}Br + CH_4$, ○, and $^{80}Br + CD_4$, ●, reactions.

explanation for these differences.

Figure 32 shows similar data for reaction with C_2H_6 and C_2D_6. About 80 experimental points for the $^{80}Br + C_2H_6$ reaction were used in drawing the best-line visual fit. Gas chromatographic analyses indicate four major organic products, CH_3Br, CH_2Br_2, C_2H_5Br, and $C_2H_4Br_2$, (or their deuterated analogs) present relative to CH_3Br in an amount 1.0, 0.17, 1.6, and 0.3 respectively.

(L. D. Spicer)

5. Liquid-Phase Hot-Atom Halogen Reactions with Halomethanes

Reaction of recoil ^{38}Cl and ^{128}I atoms with liquid chloromethanes have been studied. About 0.5 ml. samples of chloromethane containing 0.1 to 1.5 mole percent I_2 were irradiated for 4 sec. at a thermal-neutron flux of 3×10^{12} n/cm^2-sec. The samples were separated using a $CHCl_3$-aqueous Na_2SO_3 two-phase extraction and each fraction counted using a multichannel analyser. Using 0.45 MeV ^{128}I and 1.64 MeV ^{38}Cl photopeaks it was possible to determine simultaneously the percent of the ^{38}Cl or ^{128}I activity appearing as organic activity, (the organic yield, O.Y.).

The I_2-CCl_4, - $CHCl_3$, and -CH_2Cl_2 samples all exhibit a decrease in ^{38}Cl O.Y. with increasing I_2 concentration. Such behavior is characteristic of halogen scavenging action and suggests that hydrogen self-scavenging of ^{38}Cl in $CHCl_3$ and CH_2Cl_2 is not competitive with I_2. These scavenger data appear best to describe a straight line when plotted as log O.Y.

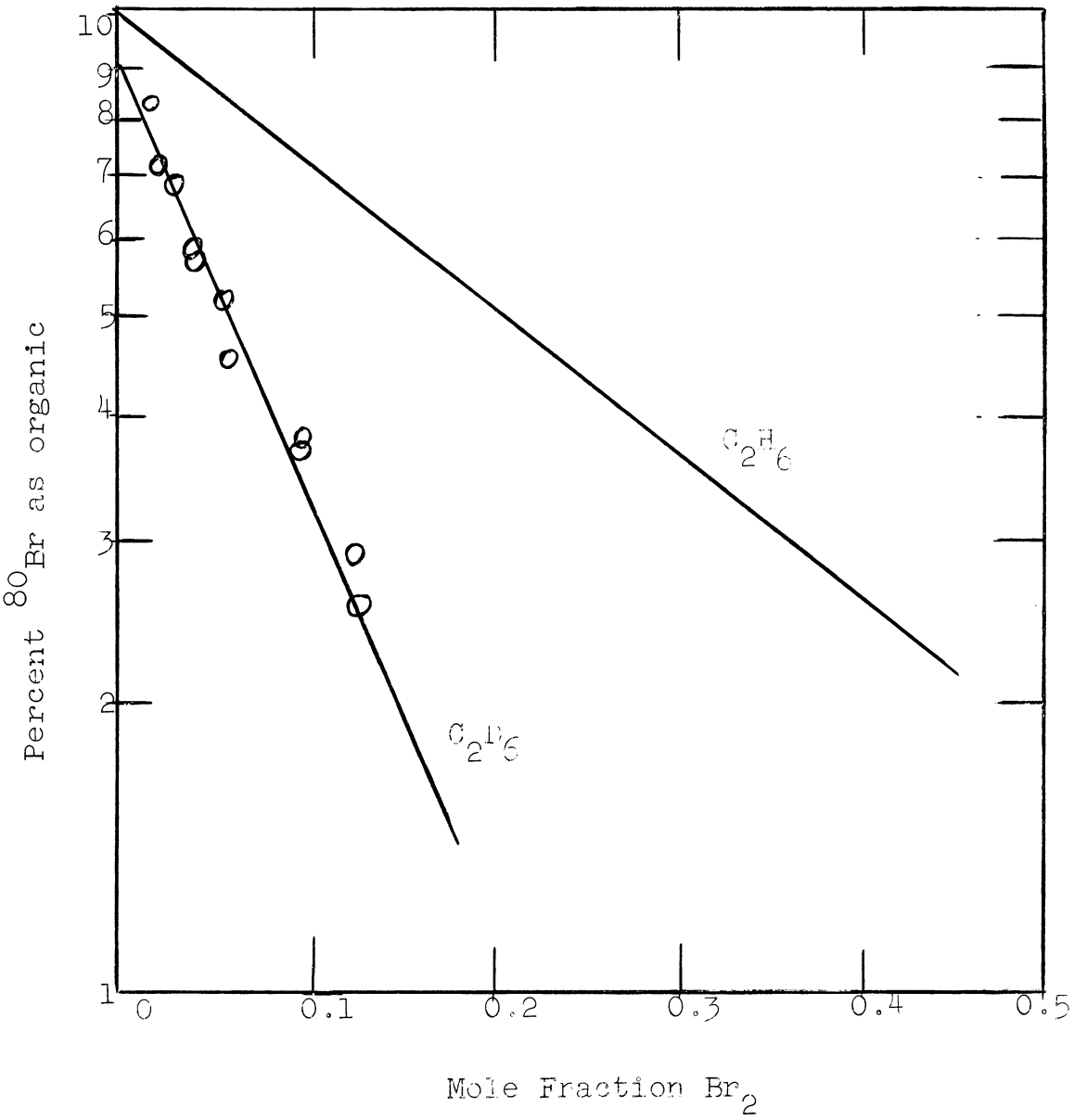

Figure 32. Percent ^{80}Br produced by (n,γ) activation which becomes stabilized as organic activity in C_2H_6 and C_2D_6.

versus mole percent I_2.

The I_2-CCl_4 data extrapolate, at zero mole fraction I_2, to 42 ± 1.0% ^{38}Cl O.Y. and 11 ± 1.5% ^{128}I O.Y. The extrapolated ^{38}Cl O.Y. is in agreement with that of Chien and Willard [J. Am. Chem. Soc., 75, 6160 (1953)] who irradiated Cl_2-CCl_4 mixtures. The I_2 scavenger curve lies slightly above the Cl_2 scavenger curve of Chien and Willard.

Similar data for I_2-$CHCl_3$ mixtures exhibit zero mole-fraction I_2 extrapolated organic yields of 437 ± 1.5% ^{38}Cl and 26 ± 1% ^{128}I. For I_2-CH_2Cl_2 the extrapolated yields are 35 ± 1.5% ^{38}Cl and 47 ± 2% ^{128}I.

(B. Gregory Gibbard)

6. Activation Analysis of Archaeological Artifacts

Chemical analyses of materials serve to provide valuable information needed in many archaeological and anthropological studies since appearances, very often, can be deceiving. For example, recent analysis of English Bronze Age artifacts have shown that some samples were in fact copper; this has resulted in the need for a reappraisal of this period of British prehistory. As another example, given a silver coin, an expert would have difficulty on the basis of appearance alone determining whether the silver contained a moderate proportion of alloy or whether it was fine silver. This is of importance showing either the existence of refining techniques, or else the deliberate debasement of the coinage. Similarly, from the composition, it is possible to determine, especially in metals, the method of manufacture, and consequently the degree of technical

competence of the culture that produced it. Metals can, for example, only be spun, cast, or wrought, within certain compositional limits which are well-known.

There are many different methods of chemical analysis, but the majority of them can be disregarded because they are destructive, and even nowadays, many archaeologists are reluctant to have their finds destroyed, even though by this destruction they can learn more about them - forgetting that archaeological excavation itself, by which the objects were uncovered, is also a destructive "experiment" that cannot be repeated.

The technique of neutron activation analysis has only recently been applied to archaeology and its problems, but it is a research tool which holds much promise for the future. Several pilot studies of this method as applied to the analysis of archaeological materials have been made in America, England, France, the Netherlands, and Japan, but the program of research just starting at The University of Michigan is planned as the first extensive and intensive use of the technique.

Irradiated samples are first analysed using multi-channel (400 channel) analysis in order to determine the gamma-ray peaks present and from their energies and decay half-lives, the elements which are in the sample. For example, many pottery samples exhibit relatively large amounts of sodium and manganese radioactivity. The sodium to manganese activity ratio can serve, in some cases, to group classes of compounds.

To date about 60 samples of various types of artifacts have been analysed. A typical set of data is given below. These nine samples were potsherds obtained from Hopewell Indian burial mounds. Eight came from Illinois and one from a Michigan mound. As seen in the tabulation, sample 5 has an appreciably different Na/Mn activity value. This sample was in fact the Michigan sample.

Sample	Na/Mn Activity Ratio Relative to Sample 1
1	1.00
2	1.17
3	1.17
4	1.48
5	3.22
6	1.44
7	1.34
8	1.47
9	1.33

(T. Abeles)

7. Computer Synthesized Hot-Atom Data

Wolfgang, et. al., [J. Am. Chem. Soc., 82, 2665 (1960), J. Chem. Phys., 39, 2983 (1963), J. Chem. Phys., 41, 2159 (1964)] have shown that tritium hot-atom reaction data appear to obey the Wigner equation for neutron thermalization.

$$\ln (1 - Y_t) = - I_t \, f_R/\alpha \qquad (1)$$

where Y_t is the total hot-atom yield, I_t is the reactivity integral and

$$I_t = \int_{E_2}^{E_1} P_t (E) \, d \ln E, \qquad (2)$$

$P_t(E)$ is the total probability of reacting per collision, f_R is the collision fraction of reactive gas R, and α is the overall average logarithmic energy loss factor. For a mixture of a reactive gas R, and an inert-gas moderator, M,

$$\alpha = f_R \alpha_R + f_M \alpha_M = f_R (\alpha_R - \alpha_M) + \alpha_M \tag{3}$$

Equations (1) and (3) lead to

$$\frac{-1}{\ln(1 - Y_t)} = \frac{\alpha_R}{I_t} + \frac{f_M \alpha_M}{f_R I_t} \tag{4}$$

Thus, it has been argued that if I_t, α_M, and α_R are constants, and if the Wigner equation is applicable to hot-atom reactions, a plot of $-1/\ln (1 - Y_t)$ versus $f_M/f_R = (1 - f_R)/f_R$ should be a straight line with intercept α_R/I_t and slope α_M/I_t. The ratio of intercept to slope is α_R/α_M. Using this method, Rosenberg and Wolfgang [J. Chem. Phys., 41, 2159 (1964)] determined such α ratios for M = He and R = C_3H_8, n-C_4H_{10}, and butene-1. Their data appear to follow a linear form when plotted according to Eq. (4).

Rosenberg and Wolfgang note in addition that internal consistency checks of the mathematical formalism are available since data for each of the products, j, which comprise the total yield could be given as

$$Y_j = \frac{f_R}{\alpha} I_j - \frac{f_R^2}{\alpha^2} K_j \tag{5}$$

or

$$\frac{Y_j \alpha}{f_R} = I_j - \frac{f_R}{\alpha} K_j \tag{6}$$

Using Eq. (3) and dividing all terms by α_M

$$\frac{Y_j\left[f_R\,\frac{\alpha_R}{\alpha_M} + f_M\right]}{f_R} = \frac{I_j}{\alpha_M} - \frac{f_R K_j}{\alpha_M^2\,(f_R\,\frac{\alpha_R}{\alpha_M} + f_M)} \qquad (7)$$

If the α_R/α_M found by using Eq. (4) is used in Eq. (7), a plot of

$$Y_j\,(f_R\,\frac{\alpha_R}{\alpha_M} + f_M)/f_R \text{ versus } f_R/(f_R\,\frac{\alpha_R}{\alpha_M} + f_M)$$

should be a straight line for each product j. The slopes are $-K_j/\alpha_M^2$ and the intercepts are I_j/α_M. Furthermore, for a compound R, it should be that

$$\sum \frac{I_j}{\alpha_M} = \frac{I_t}{\alpha_M} \qquad (8)$$

and

$$\sum \frac{K_j}{\alpha_M} = \frac{1}{2}\,\frac{I_t^2}{\alpha_M^2} \qquad (9)$$

Rosenberg and Wolfgang have illustrated that the internal consistency implied by Eqs. (7)-(9) appears to exist.

We have synthesized hot-atom data using an IBM-7090 computer. We chose a P(E) function as shown in Fig. 33 and arbitrarily defined three products A, B, and C. Choosing $r_R = 0.737$, $b_R = -1.165$, $r_M = 0.2714$, and $b_R = +1.884$ as defined in [J. Chem. Phys., 41, 1595 (1964), J. Am. Chem. Soc., 86, 2782 (1964)] we have $\alpha_R = 1.148$ and $\alpha_M = 0.3084$ as also defined in these references.

In Table 1 are two typical sets of computer data for this system. Plotted in Fig. 34 are the data for seven such sets of

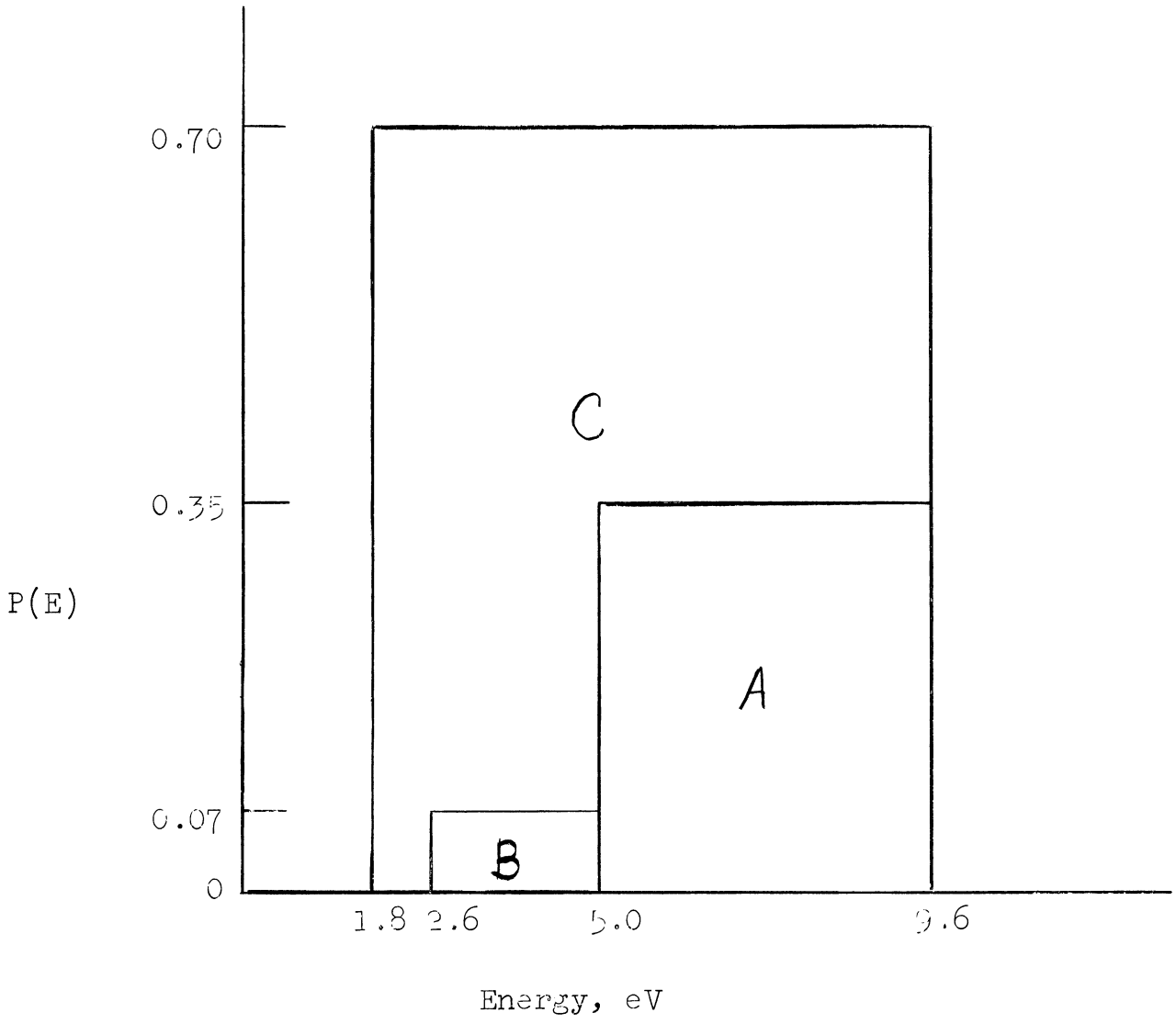

Figure 33. Arbitrarily defined reaction probability curve.

Table I. Computer Synthesized Reaction Data for Hot Atoms Produced with 2×10^5 eV Energy.[a]

Energy	$f_R = 1.00$		$f_R = 0.01$	
eV	G(E)[b]	% Reaction	G(E)[c]	% Reaction
200,000	2.69×10^{-7}	0	2.732	0
4,000	0.8731	0	3.156	0
250	0.8711	0	3.156	0
80	0.8709	0	3.156	0
30	0.8710	0	3.156	0
9.61	0.8710	0	3.156	0
8.16	0.8548	9.84	3.156	0.36
6.94	0.8155	19.37	3.153	0.72
5.89	0.7631	28.38	3.150	1.08
5.01	0.7041	36.75	3.145	1.44
4.25	0.6427	44.44	3.140	1.80
3.61	0.5816	51.42	3.134	2.16
3.07	0.5221	57.71	3.127	2.51
2.60	0.4654	63.35	3.119	2.87
2.21	0.4119	68.35	3.110	3.22
1.88	0.3619	72.77	3.101	3.58
1.60	0.3126	72.77	3.092	3.58
1.36	0.2932	72.77	3.084	3.58

a. P(E) = 0.70 in the range 1.88 to 9.61 eV.

b. For an infinite number of collisions, $G(E) = E\,F(E) = 1/\alpha = 1/1.148 = 0.8710$.

c. For an infinte number of collisions, $G(E) = E\,F(E) = 1/\alpha = 3.156$ where $\alpha = (0.99)(0.3048) + (0.01)(1.148)$.

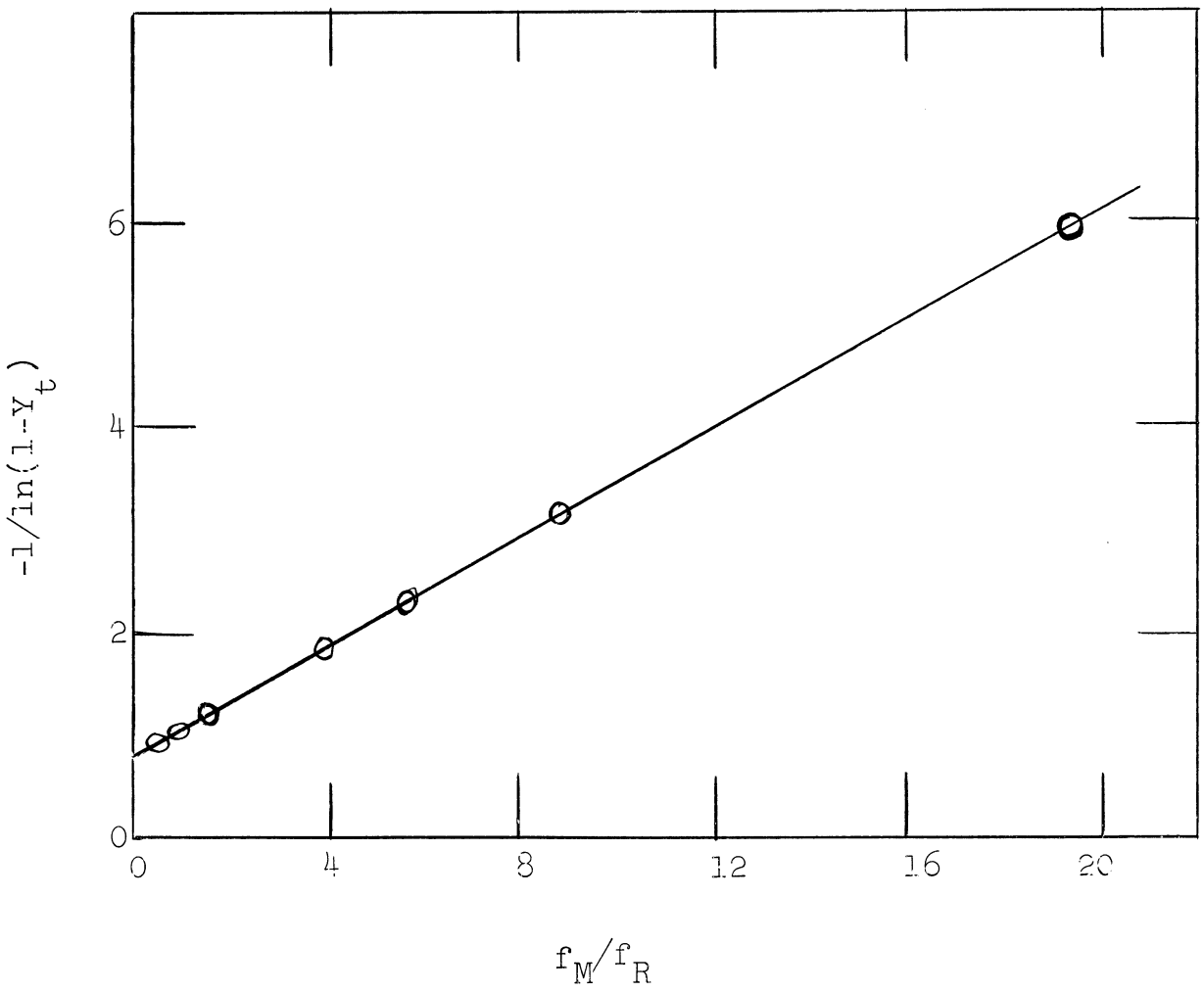

Figure 34. Plot of total yield computer data.

computer-generated hot-atom yields. As seen, Fig. 35 is a straight line with intercept $\alpha_R/I_t = 0.75$ and slope $\alpha_M/I_t = 0.27$. The ratio α_R/α_M from Fig 34 is 2.77. However, the ratio α_R/α_M used in generating these hot atom data was 1.148/0.3084 = 3.72. Thus, Fig. 34 leads to an α ratio which is 34% in error, even though a straight-line plot results.

Figure 35 are the data for products A, B, and C according to Eq. (7). Again straight lines result. For this figure,

Product	I_j/α_M	$-K_j/\alpha_M^2$
A	0.73	0.63
B	0.14	0.20
C	2.85	4.00

According to Eq. (8) $\Sigma I_j/\alpha_M = 3.72$ in excellent agreement with $I_t/\alpha_M = 1/0.27 = 3.70$. According to Eq. (9) $\Sigma K_j/\alpha_M^2 = 4.83$ which is in reasonable agreement with $I_t^2/2\alpha_M^2 = 6.75$; at least it is in no less agreement than the Rosenberg and Wolfgang experimental values.

These computer-synthesized data serve to illustrate (1) that straight-line plots are no assurance in themselves that the mathematical formulation is necessarily valid, (2) internal consistency "checks" may instill false confidence, (3) the method of plotting may lead to consistently inconsistent α_R/α_M values.

(K. Verosub)

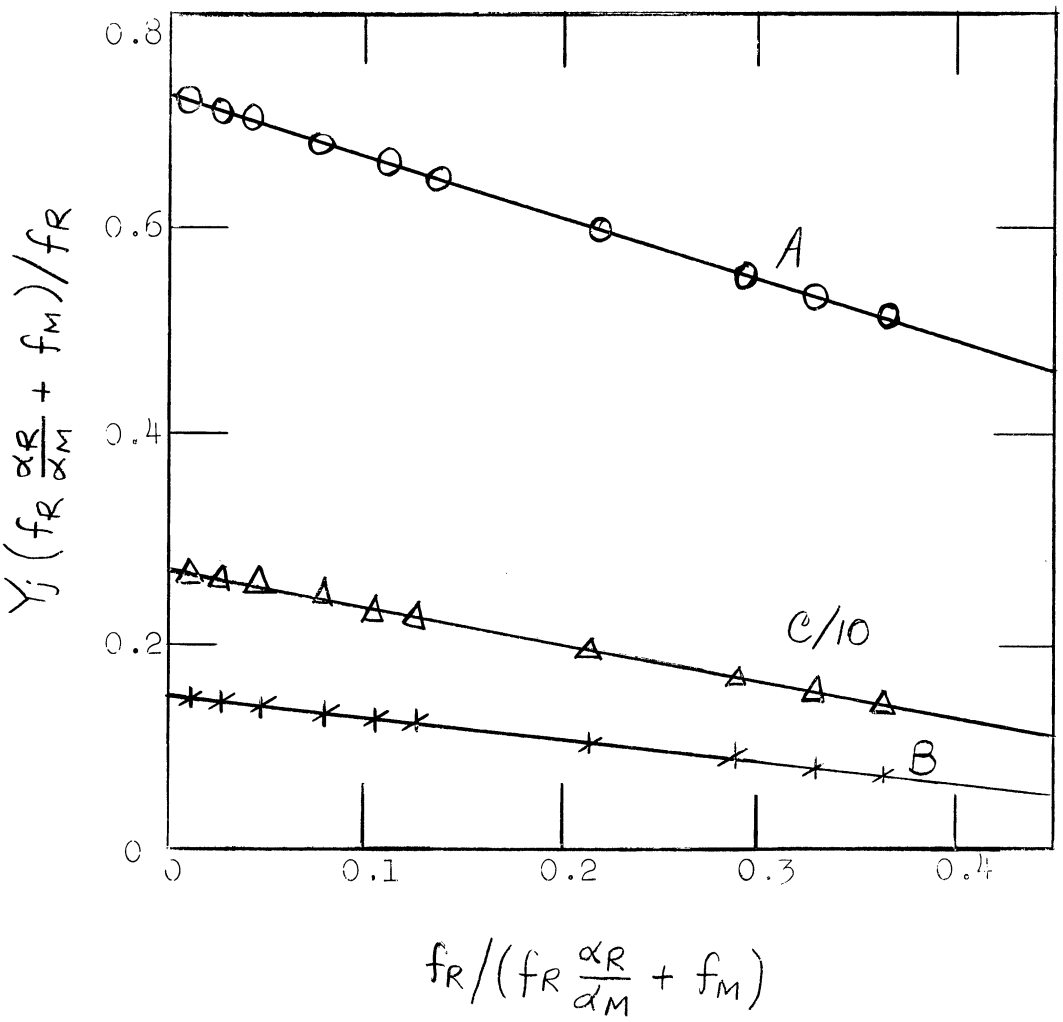

Figure 35. Plot of individual yield computer data.

8. Analog Computer Analyses

As an adjunct to the digital computer analysis described in section 7, we are attempting to synthesize hot-atom data using an analog computer. An analog computer has certain advantages over the IBM computer. Specifically, it is possible to operate the computer and immediately see (graphically) the results. If these are not of the type desired, the input parameters can be changed at once and the "calculation" repeated. We can foresee potential application of this instrument in adjusting input parameters until the synthesized data correspond to the experimentally observed hot-atom data. A disadvantage of the analog computer is the overall error of the final result. This error depends on the precision rating of the resistors and capacitors used in the circuitry.

Work during this past year consisted of building three function generators and a function multiplier.

Initial studies have been made to derive the hot-atom energy distribution function, F(E), using various forms of the differential scattering function.

(D. Pinkel, J. Ekin)

9. Fission Hot-Atom Reactions.

A few investigators have shown that uranium fission products are capable of reacting as hot atoms or ions. We are attempting to utilize this technique followed by gas chromatographic separation in order to provide a rapid method for the separation of fission products. For example, fission tellurium formed in the presence of a liquid hydrocarbon could, by hot atom reactions, results in some H_2Te. If an irradiated U-hydrocarbon sample is separated by gas chromatography, it would be possible to obtain an H_2Te sample within a minute or two following the irradiation. Multichannel gamma-peak height analysis of the H_2Te would indicate the types and amounts of Te fission isotopes.

Preliminary studies indicate that such a method is feasible. The radio-gas chromatograph illustrated in Figs. 2-5 is in its final stages of construction and experiments will be resumed in a few months.

(M. P. Tsoukatos, D. Zellmer)

PERSONNEL

1. Principal Investigator

   Adon A. Gordus

2. Postdoctoral Associate

   Emma Verdieck (part-time as of Feb. 15, 1965)

   Hans O. Denschlag (full-time as of May 1, 1965)

3. Graduate Reseach Assistants (part-time hourly)

   Thomas Abeles (part-time - Sept. 1964 - Dec. 1964, full-time as Jan. 1965).

   B. Gregory Gibbard (part-time)

   James R. Griffith (part-time as of May 1964)

   Paul B. Merrithew (part-time as of May, 1965)

   Marios Tsoukatos (part-time as of May, 1964)

4. Undergraduate Honors Research Assistants (hourly)

   Michael J. Berry (as of Sept., 1964)

   Robert Brammer (as of Dec. 1964)

   David Caughey (full year)

   Jack Ekin (as of Oct. 1964)

   William Fink (as of Dec. 1964

   Richard Gomberg (as of Sept. 1964

   John Gunkler (as of Dec. 1964)

   William Litzenberg (full year)

   Richard Pearson, Jr. (full year)

   Daniel Pinkel (as of May, 1964)

   Leonard D. Spicer [a] (graduated Aug. 1964)

   Kenneth Verosub (full year)

   David Zellmer[b] (graduated August, 1964)

[a] Present address: Department of Chemistry, Yale University

[b] Present address: Department of Chemistry, University of Illinois.

TALKS AND LECTURES

1. Two guest lectures for AEC-NSF sponsored summer institute.
2. Grand Valley State College Summer Science Program, July 20, 1964 "Activation Analysis and Reactor Research"
3. Purdue University, Nov. 13, 1964, "High Energy Chemical Reactions."
4. Ann Arbor High Schools Science Program, Nov. 14, 1964 "Neutron Activation Analysis of Archaeological Samples."
5. IAEA Symposium on Chemical Effects Associated with Nuclear Reactions and Radioactive Transformations, "Gas Phase Reactions of (n,γ) and I.T. Activated ^{80}Br with Alkanes and Haloalkanes." Dec. 7, 1964, Vienna, Austria.
6. "Bond Rupture Following ^{14}C and ^{3}T Beta Decay", IAEA Symposium, Vienna, Dec. 11, 1964.
7. Guest lectures in high-energy kinetics - Chemistry Department, U. of Michigan, Feb. 4, 9, 11, 1965.
8. Various talks on "Undergraduate Research", "Science Honors Programs", "Radioactivity Research" before all-Ohio Honors conference, U-M Alumni groups, groups at other Colleges and Universities, University groups, and high school groups.

PUBLICATIONS

1. C. H. Hsiung and Adon A. Gordus, "Neutron Thermalization Theory Applied to Hot Atom Chemical Reactions: Consideration of Isotropic and Asymmetric Scattering," J. Am. Chem. Soc., 86, 2782, (1964).
2. C. H. Hsiung and Adon A. Gordus, "Neutron Thermalization Theory Applied to Hot Atom Chemical Reactions: Consideration of Isotropic and Asymmetric Scattering, Supplementary Data" Document No. 7774, ADI Auxiliary Publications Project, Library of Congress, Washington 25, D.C.
3. C. H. Hsiung, Kenneth L. Verosub, and Adon A. Gordus, "Energy Distribution Function for Hot Atoms Produced by Nuclear Transformations," J. Chem. Phys., 41, No. 6, 1595, (1964).
4. Leonard D. Spicer and Adon A. Gordus, "Gas-Phase Reactions of (n,γ) and I.T. Activated ^{80}Br with Alkanes and Haloalkanes," to be published in the Proceeding of the IAEA Symposium on the Chemical Effects of Nuclear Reactions and Radioactive Transformations, Dec. 7-11, 1964, Vienna Austria.
5. C. H. Hsiung and Adon A. Gordus, "Bond Rupture Following ^{14}C and ^{3}T Beta Decay," IAEA Proceedings.

In Preparation

1. Ultraviolet Absorption Spectra of HI, DI, and HBr, DBr.
2. Gas Chromatographic Separation of CH_4 and C_2H_6 Isotopically-Labeled Molecules.
3. Activation Analysis Applied to Archaeological Artifacts.